rRNA Disruption: A Predictive Marker of Response to Taxane Chemotherapy

by

Rashmi Narendrula

A thesis submitted in partial fulfillment
of the requirements for the degree of
Master of Science (MSc) in Biology

The School of Graduate Studies
Laurentian University
Sudbury, Ontario, Canada

THESIS DEFENCE COMMITTEE/COMITÉ DE SOUTENANCE DE THÈSE

Laurentian Université/Université Laurentienne
School of Graduate Studies/École des études supérieures

Title of Thesis Titre de la thèse	rRNA DISRUPTION: A PREDICTIVE MARKER OF RESPONSE TO TAXANE CHEMOTHERAPY
Name of Candidate Nom du candidat	Narendrula, Rashmi
Degree Diplôme	Master of Science
Department/Program Département/Programme	Biology
Date of Defence Date de la soutenance	December 19, 2013

APPROVED/APPROUVÉ

Thesis Examiners/Examinateurs de thèse:

Dr. Carita Lannér
(Co-supervisor/Co-directrice de thèse)

Dr. Amadeo Parissenti
(Co-supervisor/Co-directeur de thèse)

Dr. Mazen Saleh
(Committee member/Membre du comité)

Dr. Kenneth P. Nephew
(External Examiner/Examinateur externe)

Approved for the School of Graduate Studies
Approuvé pour l'École des études supérieures
Dr. David Lesbarrères
M. David Lesbarrères
Director, School of Graduate Studies
Directeur, École des études supérieures

ACCESSIBILITY CLAUSE AND PERMISSION TO USE

Abstract

A recent clinical trial for locally advanced breast cancer patients treated with epirubicin and docetaxel prior to surgery reported significant dose-dependent reductions in tumour RNA integrity values which correlated with pathological complete response. The purpose of the present study was to assess whether similar chemotherapy-dependent alterations in RNA integrity could occur *in vitro* and to assess its relationship, if any, to apoptosis. Treatment of wildtype A2780 ovarian carcinoma cells with taxanes resulted in dose- and time-dependent RNA degradation, identified as several unique bands on electropherograms having mobilities lower than the 28S and 18S rRNAs. We refer to this chemotherapy-dependent generation of aberrant RNA bands on electropherograms as "RNA disruption". RNA disruption was found to be temporally associated with the induction of apoptosis, as determined by the appearance of a sub G1 peak of DNA content, positive annexin-V staining, and both PARP-1 and caspase-3 cleavage. Treatment of cells with a caspase-3 inhibitor resulted in a significant reduction in rRNA disruption, suggesting the involvement of caspase-3 or related caspases in RNA disruption. In contrast, docetaxel-dependent rRNA disruption was absent when docetaxel was administered to docetaxel-resistant A2780DXL cells, indicating that changes in RNA integrity may possibly differentiate between responsive and non-responsive tumours in cancer patients.

Acknowledgments

I would like to take this opportunity to thank the following individuals for their help throughout my thesis. First and foremost, my supervisors Dr. Carita Lanner and Dr. Amadeo Parissenti, for giving me the opportunity to work with them and for all their support and guidance throughout this research project. I would also like to thank Dr. Mazen Saleh, a member of the supervisory committee, for providing valuable feedback and Dr. Eric Gauthier for suggesting some techniques to use when designing experiments to study apoptosis. I would also like to take this opportunity to thank Northern Ontario School of Medicine and RNA Diagnostics Inc. for providing the funding necessary to carry on this project. Next, I would like to thank Dr. Baoqing Guo for teaching me how to use the Bioanalyzer and analyze the results, and to the other members of Parissenti lab and colleagues at the Northern Ontario School of Medicine lab for their critical feedback, help and encouragement in completing this research project. Finally, I would also like to thank my friends and family for their constant support, love and encouragement.

Table of Contents

List of Figures

1.0 Introduction

1.1 Taxanes in Chemotherapy

1.1.1 History

Taxanes are one of the most commonly used chemotherapy agents, applied in the treatment of a wide range of tumours. They are derived from the yew tree of genus *Taxus.* As part of the National Cancer Institute's program (1962) to evaluate plants for antitumour activity, crude bark extracts were obtained from the Pacific yew tree, *Taxus brevifolia* and found to be cytotoxic against several murine tumours [1]. In 1971, the active ingredient in the extract found to have antitumour activity was identified as paclitaxel [2]. Due to the difficulty in obtaining sufficient quantities of paclitaxel and the high costs involved in extraction, paclitaxel is presently derived in a semi-synthetic form from chemicals derived from the needles of *Taxus baccata* [3]. Horowitz and colleagues reported tubulin polymerization and stabilization of microtubules as the mechanism of action of paclitaxel in 1979 [1]. Paclitaxel entered clinical trials in 1983, the results of which identified the drug as an effective anticancer agent for treating cancers, in particular ovarian and metastatic breast cancer [4]. As paclitaxel is insoluble in water, docetaxel, which is a semisynthetic analog of paclitaxel with higher water solubility, was the second taxane to enter clinical trials in 1986 [2].

Currently, in the clinic, taxanes are being used alone, following another drug regiment, or in combination with other drugs to treat several types of cancers [5]. Paclitaxel, one of the most effective anti-neoplastic drugs currently available, is used in the treatment of breast cancer, ovarian cancer, non-small cell lung cancer and AIDS-related Kaposi's Sarcoma[6]. Docetaxel is active against several solid tumours including breast, gastric, ovarian and non-small cell lung cancer [7]. Further research is being conducted to test both docetaxel and paclitaxel in the

treatment of other types of cancers. A treatment regimen for ovarian cancer consisting of a taxane and a platinating agent reported that docetaxel resulted in an improved quality of life for the same length of progression free survival which identified docetaxel as an improved alternative for paclitaxel in ovarian cancer treatment [8, 9].

1.1.2 Current clinical use in Breast and Ovarian Cancer

Breast cancer is the second most commonly diagnosed cancer in the world, with approximately 1.38 million new cases diagnosed in 2008 [10]. It is the leading cause of cancer-related death among females worldwide [11]. Treatment for breast cancer patients depends on the type and stage of cancer, and may involve surgery, radiation therapy, chemotherapy, hormone therapy or targeted therapy. Adjuvant chemotherapy (following surgery) consisting of a taxane and an anthracycline has been associated with reduced risk of relapse and death among women with operable breast cancer, with paclitaxel resulting in improved disease free survival and overall survival compared to docetaxel when administered in combination with doxorubicin and cyclophosphamide[12]. For advanced breast cancers, including locally advanced breast cancer, chemotherapy may be administered prior to surgery (neoadjuvant chemotherapy) [13].

The eighth most common malignancy among women worldwide is ovarian cancer, resulting in more than 140 000 deaths [14]. It is the sixth most common cancer in terms of mortality and incidence in the developed countries, with a 5-year mortality rate of greater than 50% [15]. These high mortality rates may be attributed to diagnosis at an advanced stage of the disease and to the development of resistance to treatment. Treatment for ovarian cancer consists of debulking surgery followed by adjuvant chemotherapy with carboplatin plus a taxane [16]. Initially, the taxane of choice to treat ovarian cancer was paclitaxel, but due to the manageable toxicities observed, docetaxel may be used in combination with carboplatin when treating

patients [8]. In some instances, particularly where primary debulking surgery is not suitable for ovarian cancer patients, neoadjuvant chemotherapy may be considered as a treatment option for patients suffering with advanced disease [17]. As well, taxanes may be used in the case of recurrent disease for treatment of patients where surgery is not feasible or where platinum resistance is established [18-20].

1.2 Biological Effects of Taxanes

1.2.1 Mechanism of Action

Taxanes are cytotoxic drugs that interfere with microtubule depolymerization, causing cell cycle arrest and cell death via apoptosis [21]. Microtubules are protein polymers composed of α and β-tubulin heterodimers, that are important in maintaining cell shape, allowing for cellular signalling and movement as well as facilitating cell division [22]. Taxanes tightly bind to β-tubulin monomers in the microtubules, preventing depolymerization of microtubules, which results in an arrest of the cell cycle [23]. Comparing the two taxanes, docetaxel is reported to have 1.9 fold higher affinity for the β-tubulin binding site compared to paclitaxel [23].

Cell death pathways triggered as a result of treatment with taxanes are not completely understood. Research indicates that the apoptotic pathway is activated as a result of taxane chemotherapy treatment through modulation of Bcl-2 (B-cell lymphoma 2). Bcl-2 is an apoptotic regulator protein that suppresses apoptosis. Some reports have indicated that treatment with taxanes reduces cellular levels of Bcl-2 (an inhibitor or apoptosis) through inhibition of *BCL2* gene transcription [24], where as others have observed an increase in phosphorylation of Bcl-2, which results in loss of function of the protein and promotes apoptosis [25]. Although the changes in Bcl-2 as a result of taxane treatment are unclear, it has been observed that due to the higher affinity of docetaxel for the β-tubulin subunit, enhanced Bcl-2 phosphorylation is

observed at lower concentrations of docetaxel when compared to paclitaxel [26]. The activation of caspases, cysteine-aspartic proteases, results in the cleavage of other protein substrates within cells, a molecular mechanism that is characteristic of apoptosis. In some cell lines (lung, ovarian, thyroid, prostate and breast), cleavage of caspase-8, -9 and the subsequent cleavage of caspase-3 and PARP (Poly-ADP ribose Polymerase) have been identified as the main executioners of apoptosis when cells are treated with taxanes [5]. However, taxanes have also been shown to induce caspase-independent cell death pathways, both *in vitro* and *in vivo*, due to variations in dose, tumour microenvironment and cell type [27].

Taxane cytotoxicity can also occur as a result of increased TNF-α production, as observed in multiple cancer cell lines [28]. An earlier study published in 1992, reported that Taxol triggered increased production of TNF-α by inflammatory murine macrophages [29]. Tumour-necrosis factor (TNF)-α is a pleiotropic cytokine produced mainly by activated monocytes or macrophages, that exists as a membrane – bound (mTNF-α) and a soluble form (sTNF-α) [30]. TNF-α signal transduction occurs through two transmembrane receptors, TNFR1 and TNFR2, to regulate cell differentiation, proliferation and apoptosis [31]. Binding of TNF-α, either the membrane – bound or soluble form, to TNFR1, which possesses a death effector domain (DED), promotes apoptosis through cleavage of caspase-8, whereas binding to TNFR2, which lacks a DED, promotes NF-κB activity and induces the expression of survival genes [32]. A study investigating treatment of breast and ovarian cancer cell lines (MCF-7 and A2780 respectively) with both paclitaxel and docetaxel reported dose-dependent increases in the production of sTNF-α, which may contribute to the cytotoxic effect of taxanes observed in cancer cell lines through the activation of TNFR1-induced apoptosis [28].

Several other mechanisms have been identified that may explain how taxanes inhibit tumour growth both *in vivo* and *in vitro*. Reactive oxygen species (ROS) are highly reactive oxygen molecules that are extremely harmful at high concentrations as they readily react with and damage DNA, RNA, proteins and lipids, which may result in cell death [33]. An *in vitro* study investigating the effects of docetaxel on hepatocellular carcinoma cells reported a dose-dependent increase in ROS levels with treatment, which may contribute to the toxicity of docetaxel [34]. Formation of a neovascular blood supply, by angiogenesis, is crucial for the propagation of tumours. Taxanes have been reported to inhibit angiogenesis by down regulation of vascular endothelial growth factor (VEGF) or through endothelial cell necrosis, resulting in the inhibition of endothelial cell proliferation, migration, and tube formation [35]. This may in turn reduce tumour growth by reducing nutrient and oxygen availability to the tumour.

1.2.2 Mechanisms of Resistance

Taxanes are used to treat a wide range of cancers; however, one of the persistent problems associated with the use of taxanes is the development of drug resistance and the subsequent lack of response to treatment. The mechanism of development of drug resistance has been well studied and characterized for taxanes, and avoiding this process is crucial to obtaining clinical success when taxanes are used for chemotherapy.

Some of the mechanisms involved in taxane resistance *in vitro and in vivo* have been identified, although, as is the case for other chemotherapy treatments, resistance to taxanes may be multifactorial and is yet to be fully understood. One of the proposed mechanisms of resistance to taxanes involves alterations in microtubule structures. A study by Kavallaris et al., reported increased expression of β-tubulin isotypes in Taxol resistant cells lines and human tumours, suggesting the importance of changes in specific β-tubulin gene expression in contributing to

resistance [36]. A clinical study investigating the mechanism of resistance in non small cell lung cancer patients, identified the presence of missense mutations of the β-tubulin gene in tumour DNA isolated from patients which conferred resistance to paclitaxel treatment [37]. Based on these studies, it appears that alterations in β-tubulin, either by increased expression or by mutations in the gene, can affect binding of taxanes to the β-tubulin subunit, which may lead to resistance to taxane chemotherapy.

Since taxanes have been associated with induction of apoptosis, another mechanism of taxane resistance is the increased expression of anti-apoptotic genes. In a study investigating the sensitivity of MCF-7 breast cancer cells to taxanes, it was observed that over expression of the anti-apoptotic genes coding for Bcl-xL and c-FLIP resulted in sensitivity of cancer cells to taxanes [38]. Since Bcl-xL inhibits the intrinsic pathway, and c-FLIP inhibits the extrinsic pathway of apoptosis, the results from this study suggest that over expression of these genes results in increased survival of cancer cells. Survivin, which belongs to the inhibitor of apoptosis protein (IAP) family, is another anti-apoptotic protein which is highly expressed in some cancers, but is undetectable in normal adult tissue, and can block both caspase-dependent and independent death pathways [39]. Increased survivin expression in transfected human ovarian carcinoma cell lines (IGROV-1 and OAW42), as well as increased protein expression in advanced ovarian carcinoma patients have been significantly associated with resistance to Taxol [40].

Another common mechanism of taxane resistance identified in preclinical studies is the increased expression of P-glycoprotein (P-gp) efflux pumps. P-gp, a product of multidrug resistance gene-1 (MDR-1), belongs to the ATP-binding cassette (ABC) family of drug transporters located on the plasma membrane [21]. These drug transporters are responsible for

the ATP dependent efflux of various chemotherapy drugs from tumour cells, including taxanes [41]. In MCF-7 cells that were selected for survival in increasing concentrations of docetaxel, *ABCB1* gene amplification was observed upon acquisition of docetaxel resistance [42]. Using microarray analysis and Q-PCR, Armstrong et al. reported a significant increase in the expression of the *ABCB1* and *ABCB4* genes in A2780DXL cells, a docetaxel resistant ovarian cancer cell line [43]. Similar observations were made in paclitaxel-resistant SKOV-3 and OVCAR ovarian cancer cell lines, where upon the inhibition of ABCB1 expression paclitaxel sensitivity was restored [44]. An association between ABCB1 expression and resistance to chemotherapy was also established for breast cancer patients undergoing paclitaxel treatment, where the presence of a certain ABCB1 genotype resulted in chemoresistance and shorter overall survival [45].

Another mechanism of resistance to taxanes has been identified that involves increased expression of enzymes capable of metabolizing taxanes. Cytochrome P450 enzymes are involved in the metabolism of several anticancer agents, including taxanes. CYP2C8, a member of the Cytochrome P450 superfamily of proteins, has been shown to detoxify paclitaxel to a metabolite that is approximately 30 fold less cytotoxic product [46]. CYP1B1 has been identified in many malignant tumours, and it has been shown that its increased expression is associated with metastatic disease [47]. A study investigating *CYP1B1* polymorphisms and response to docetaxel treatment in castration-resistant prostate cancer patients, found an association between increased expression of this cytochrome P450 enzyme and lower response rate to the treatment [48].

Another mechanism of resistance identified for taxanes is the activation of Tumour Necrosis Factor Receptor 2 (TNFR2). TNFR2 lacks a death domain and it has been shown that TNF-α induced expression of TNFR2 is associated with increased proliferation of colon cancer cells

[49]. In a study by Sprowl et al, acquisition of resistance to taxanes was associated with increased survival as a result of TNFR2 activation and NF-κB activity [28]. Moreover, the study showed that when an inhibitor of NF-κB was used to treat the resistant cells, sensitivity to docetaxel was re-established in docetaxel resistant breast and ovarian cancer cells.

1.3 Characterization of Response to Taxanes

1.3.1 *In vitro* Markers

Treatment of cancer cells with taxanes (alone or in combination with other chemotherapy agents) results in the activation of several pathways within cells. Several biomarkers have been observed to change *in vitro* as a result of treatment with taxanes.

Binding of taxanes to β-tubulin subunits prevent depolymerization of microtubules, inhibiting the dynamic reorganization of microtubule network that is essential for proper cell division. Due to stabilized microtubules, treatment with taxanes have been reported to cause an arrest in the G2/M phase of the cell cycle [50]. This is a characteristic response that is observed as a result of treatment with taxanes in many cancer cells, as they are dividing at a much higher rate than normal cells and are therefore more susceptible [51]. The mitotic bundles that form as a result of interaction between taxanes and microtubules, along with inhibiting their depolymerization, have also been reported to impair centromere dynamics [52]. This study used a labeled centromere binding protein to investigate the effect of paclitaxel on human osteosarcoma cells. It was reported that concentrations of paclitaxel which resulted in blocked mitosis, also suppressed the rates of stretching and relaxation of sister centromere pairs and significantly reduced the distance between centromeres, suggesting it as a possible mechanism by which mitosis is inhibited by taxanes. In a study investigating chemotherapy naive and resistant breast cancer cell lines, it was reported that treatment with paclitaxel resulted in G2/M

cell cycle arrest in a sensitive cell line but not the resistant cell line [53]. This validates the use of cell cycle arrest in the G2/M phase as an *in vitro* marker to indentify response to taxane chemotherapy.

Another characteristic response of cells treated with taxanes is the occurrence of multinucleation. Multinucleation is a morphological indicator of mitotic catastrophe, a phenomenon characterized by impaired chromosome segregation and formation of nuclear envelope around individual or groups of chromosomes, resulting in the formation of large multinucleated cells [54]. Cells undergoing mitotic catastrophe are multinucleated, and are distinct from apoptotic cells, which are small cells with condensed chromatin and fragmented nuclei (compared to multinucleated cells with large uncondensed nuclei). Although the cell death mechanisms induced by taxanes are not fully understood, some have argued that mitotic catastrophe, rather than being a distinct cell death pathway, is a process that precedes necrotic or apoptotic pathways [55]. In a review article by Roninson et al., mitotic catastrophe was identified as a prominent cell death pathway in response to Taxol [56]. Multinucleation was observed in human breast cancer cell lines (MDA-MB-468 and MCF-7) as a result of paclitaxel treatment [57]. This report proposed that paclitaxel induced microtubule disruption causes cell cycle arrest and prevents cytokinesis which causes the formation of multinucleated cells. Similar results were observed for MCF-7, MCF-10A and MDA-MB-231 breast cancer cells treated with docetaxel [54].

Treatment with taxanes has been associated with G2/M arrest and appearance of a multinucleated morphology; however, several gene and protein expression changes have also been observed *in vitro*, and may be used to determine if cells are responding to taxanes. Low levels of Bcl-2, an anti-apoptotic marker, has been associated with a response to docetaxel and

paclitaxel treatment in prostate, breast and lung cancer cell lines [24]. Another article published in 2010, identified cells expressing Bad, a pro-apoptotic protein, as more sensitive to taxane chemotherapy in various breast cancer cell lines [58]. This study suggested that although Bad did not induce taxane treatment dependent apoptotic pathways, cell death occurred indirectly as a result of stimulation of cell proliferation due to Bad expression. Since rapidly dividing cells are targeted by taxanes, Bad expression can serve as a marker of taxane sensitivity and response.

Over expression of MAP2, microtubule associated protein 2, as observed in several types of cancer, has also been positively correlated ($R^2 > 0.99$) with paclitaxel sensitivity in MCF-7 cell line [59]. MAP2 binds to and stabilizes microtubules, thus enhancing interaction with paclitaxel, thereby contributing to drug sensitivity.

Identifying biomarkers *in vitro* becomes complex as variation in drug dose and treatment time results in the activation of different pathways in cells, and may be affected by the unique genetic makeup of different cell lines being investigated. Several studies have been conducted, such as the one by Ferriss et al., to identify biomarkers of response to paclitaxel, *in vitro* and in patients, in an effort to differentiate responders to treatment from non responders [60].

1.3.2 Clinical Detection and Measurement

Despite the clinical success obtained by using taxanes, resistance, either innate or acquired, results in poor prognosis. Although the initial clinical complete response rate for ovarian cancer patients is greater than 50% for first line therapy, many of the responders ultimately relapse and develop resistance [61]. It is therefore crucial to differentiate between tumours that are responding to treatment versus those that are not, in both the neoadjuvant and recurrent disease setting where samples can be obtained from biopsies or ascities collected, in order to effectively treat patients. In contrast to cells cultured *in vitro*, cancer cells in patients

have a slower doubling time, therefore, the clinical activity of taxanes may not be a result of the antimitotic effect of taxanes alone [62]. Thus it is essential to understand how response to taxanes can be measured in a clinical setting to provide patients with an overall survival benefit.

For solid tumours, response to treatment is evaluated based on the Response Evaluation Criteria in Solid Tumours (RECIST) into four categories: complete response, partial response, stable disease and progressive disease based on the size of measurable lesions[63]. Complete response indicates all of the cancer or tumour has disappeared and no evidence of disease is present, whereas partial response indicates the tumour has shrunk but still remains, as detected by palpation of by imaging approaches. If the cancer has neither increased nor shrunk in size, it is considered a stable disease. Disease progression indicates an increase in the size of the tumour, meaning that the tumour has grown more than before treatment [64]. When assessing clinical trials, terms such as overall survival (OS) and progression-free survival (PFS) are used to describe treatment outcome and prognosis. Overall survival indicates the percentage of patients who have survived for a defined period of time since treatment that have not died from any cause, whereas progression-free survival is defined as the time following treatment, when the disease remains stable without any progression or death from any cause [65]. Another end point for survival that can be used in clinical trials is disease-free survival (DFS), which is defined as the length of time after primary treatment to the recurrence of that cancer [66]. Another prognostic term that is used to describe response to treatment in patients is pathological complete response (pCR), which is defined as the absence of any residual invasive tumour cells as assessed microscopically by a pathologist in the original tumour site and the absence of metastasis [67].

1.3.3 Methods to Measure Clinical Response

In vitro measurement of response to treatment is characterized using morphological and molecular markers, where as in patients, other methods e.g RECIST as well as other markers (CA125, PSA) are used to measure response to therapy. Initially, treatment response in solid tumour is evaluated by measuring tumour size prior to and following treatment using palpation and calipers [68]. Diagnostic imaging is another non-invasive method of measuring the effect of treatment on tumour size. Computerized tomography (CT), ultrasound and magnetic resonance imaging (MRI) are currently used to obtain accurate and reliable information regarding tumour growth or shrinkage [69]. Positron Emission Scanning (PET) is another commonly used imaging technique that uses radiopharmaceuticals to obtain images of the distribution of a radioactive tracer being used. The most commonly used radio tracer for oncological application is fluorine-18 coupled with glucose, fluorodeoxyglucose (FDG), which is essentially metabolized in the body similar to glucose. As tumour cells have very high glucose utilization, by using (FDG) PET, reduction in tumour FDG uptake in patients as a result of the growth arrest or death of tumour cells by chemotherapy agents can be used to assess treatment response [70]. Although non invasive imaging techniques can provide useful information regarding response based on changes like size and metabolic activity, limitations arise due to reduced sensitivity of some techniques in detecting small lesions or slow growing tumours, characteristic of chemotherapy resistant cells [71].

1.3.4 Methods to Obtain Clinical Biopsies for the Measurement of Biomarkers of Clinical Response

Depending on where the tumour is, different methods can be used to obtain biopsies from tumour. Needle biopsies such as a fine needle aspiration biopsy (FNAB) are obtained using thin

hollow needles and a small syringe to obtain small amounts of fluids and cells from a tumour site. In core biopsies, large needles, typically attached to a biopsy gun are used to obtain a cylinder of intact tissue [72]. Surgical approaches can also be used to obtain an excisional biopsy (where the entire lesion is removed) or an incisional biopsy (where only a small sample amount of tissue is removed) [73]. By obtaining tumour samples, physicians are not only able to make a diagnosis, but are also able to obtain vital information regarding the molecular characteristics of a tumour and monitor response to treatment by obtaining biopsies during the course of treatment.

1.3.5 Molecular Markers of Response Detection

Cancer antigen 125 (CA125) has been identified as an important diagnostic marker for ovarian cancer patients. It is a high molecular weight glycoprotein, which is highly expressed in the tumours of a large proportion of ovarian cancer patients [74]. However, since not all women with ovarian cancer show elevated tumour CA125 expression, it cannot be used a definitive marker for response to chemotherapy. Expression of the estrogen receptor (ER) and progesterone receptor (PR) are widely used biomarkers in breast cancer patients as an indicator of sensitivity and response to endocrine treatment [75]. Endocrine therapy targets hormone signaling, either by affecting estrogen and progesterone receptors, or by inhibiting the synthesis of these hormones. Estrogen and progesterone bind to the receptors on tumour cells to trigger cell proliferation; therefore, using endocrine therapy to block the activity of these hormones will stop breast tumour cell growth [76]. Human epidermal growth factor receptor 2 (HER2/neu) has also been validated as a predictor of response to HER2 targeting therapy in breast cancer [77]. HER2/neu is a proto-oncogene that is over expressed in 10 - 34% of invasive breast cancers [78]. Increased expression of HER2/neu is associated with cell growth, survival and differentiation; therefore, trastuzumab, a recombinant monoclonal antibody against HER2/neu, is used to treat breast

cancer patients with tumours that over express the HER2/neu oncogene [79]. However, since a large percent of cancers do not express these receptors, other biomarkers need to be identified that predict response to cytotoxic chemotherapy agents.

Several studies have been conducted in an effort to identify molecular markers to identify and predict response to chemotherapy in patients in order to obtain prognostic information. A recent study has shown that high expression of transducin-like enhancer of split 3 (TLE3) is associated with sensitivity to taxane chemotherapy in breast, lung and ovarian cancer patients [80]. TLE3 is a transcriptional repressor that has been shown to interact with Wnt pathway. Since aberrant Wnt signaling has been shown to impact chromosome segregation and spindle orientation, it has been proposed that TLE3 can act as an indicator of Wnt pathway activity. Over expression of p53, a tumour suppressor gene, has been shown to correlate with pCR in breast cancer patients undergoing anthracycline and taxane based chemotherapy, and has thus been identified as an indicator of response to treatment [81]. Since normal expression of p53 induces cell cycle arrest and repairs damage to DNA, the over expression of p53 observed in some breast cancer cells is possibly associated with loss of normal function and accumulation of DNA damage, resulting in cell death due to chemotherapy. However, because expression of TLE3 and p53 may vary between tumour types and patients, this has to be taken into account, before they can be used as biomarkers to monitor response to taxane based chemotherapy. At present there are no definitive markers that can differentiate tumours that are responding to treatment from those that are resistant and non-responsive.

Recently, the CAN-NCIC-MA22 clinical trial involving locally advanced breast cancer patients undergoing treatment with an anthracycline (epirubicin) and a taxane (docetaxel) were analyzed to detect biomarkers that could be associated with response to treatment [82]. In this

study, though biomarkers such as estrogen receptor, progesterone receptor and HER-2/NEU protein status were assessed, it was found that patients that exhibited pCR often contained degraded RNA, including rRNA. This study also reported dose-dependent reductions in tumour RNA integrity (RIN) values in response to treatment, establishing an association between degradation of RNA and positive patient response to treatment.

1.4 RNA Degradation in Response to Cytotoxic Agents

Cellular RNA is highly stable, and its transcription and degradation are under many levels of control [83]. RNA-degrading enzymes called ribonucleases (RNases) interact with co-factors such as helicases, polymerases and chaperone proteins, to specify the degradation of messenger RNA (mRNA), transfer RNA (tRNA) and ribosomal RNA (rRNA), which are highly controlled processes. As turnover of mRNA is crucial for regulation of gene expression, and due to the distinct inherent half-life of all RNAs, RNA degradation must be carefully controlled to recognize target RNA in order to maintain certain levels of functional RNAs within cells, while removing defective RNA molecules [83]. RNA degradation, in particular degradation of 28S rRNA into distinct fragments, has been observed in rat myeloid leukemia cells and was found to coincide with DNA fragmentation, a hallmark of apoptosis [84]. The association between RNA degradation and apoptosis was also observed in oat cells, undergoing cell death as a result of exposure to a host-specific toxin, victorin, produced by the fungus *Cochliobolus victoriae* [85]. As a result of apoptosis induction in developing rat cerebellum, degradation of both 28S rRNA and 18S rRNA was observed with DNA fragmentation, demonstrating yet again that rRNA degradation occurs together with apoptosis induction [86]. However, in mice thymoma cell lines treated with a calcium ionophore, rRNA degradation was observed in the absence of caspase activation and in a Bcl-2 independent pathway, indicating that apoptosis is not necessary for

RNA degradation to occur [87]. Although rRNA degradation has been associated with apoptosis inducing agents, its association with other cytotoxic agents such as chemotherapy has not yet been described.

In 1998 Jordan et al., reported that cisplatin, a platinating agent, inhibited ribosomal RNA synthesis *in vivo* [88]. A recent study by Burger et al., investigating the effect of several chemotherapy agents on ribosome biogenesis revealed that a large panel of chemotherapeutic drugs interfere with and inhibit rRNA synthesis at the level of transcription or processing [89]. Although there is some evidence of chemotherapy agents interfering with synthesis of rRNA, the observations made in the clinical trial by Parissenti et al. is currently the only available study showing a relationship between chemotherapy agents and RNA degradation *in vivo* [82].

1.5 Study Design and Hypothesis

Currently there are no reliable biomarkers available to differentiate between patients with tumours that respond to chemotherapy agents from patients with tumours that do not. Based on the observations made by Parissenti et al, the purpose of the present study was to develop an *in vitro* model system to study taxane-induced rRNA disruption using the A2780 ovarian cancer cell line and to determine whether this phenomenon is associated with an apoptotic response.

We hypothesize that docetaxel and paclitaxel will induce dose- and time- dependent RNA disruption in the drug sensitive A2780 cell line. We also hypothesize that biomarkers associated with apoptosis activation are elevated when RNA disruption is being observed in response to docetaxel treatment, suggesting an association between the two phenomena. Since RNA degradation occurs in response to treatment, we also hypothesize that docetaxel-induced RNA disruption will not be observed in the docetaxel-resistant A2780DXL cell line. It is further

proposed that RNA degradation could be incorporated into clinical practice to be used as an effective biomarker for positive response to taxane chemotherapy.

2.0 Methods

2.1 Cell Culture

The human ovarian carcinoma cell line (A2780) was purchased from the European Collection of Cell Cultures (ECACC, Salisbury, UK). The docetaxel resistant (A2780DXL) cell line was developed in the laboratory of Dr. Carita Lanner by culturing the parental A2780 cells in increasing concentrations of docetaxel as described in a previous study [43]. The A2780 and A2780DXL cell lines were cultured in RPMI-1640 medium containing 10% FBS, 1% penicillin (10,000 units/mL), 1% streptomycin (10,000 units/mL) (Hyclone Laboratories, Logan UT) and 0.05% gentamicin sulfate solution. The flasks were incubated in a humidified incubator at 37 ^{o}C with 5% CO_2. Resistance to docetaxel in the A2780DXL cell line was maintained by adding 4.05×10^{-7} M docetaxel to the medium weekly.

2.2 Determination of Dose and Time Response – Treatment with Docetaxel

a. Dose Response

Cells were plated at a density of 500 000 cells/well in a 6 well plate and incubated at 37 ^{o}C with 5% CO_2. Following 24 hr, RNA extraction and cell count were performed for the 0 hr wells. Remaining culture wells were treated with 2 mL of media containing the following docetaxel (DXL) concentrations: 0 μM, 0.001 μM, 0.005 μM, 0.01 μM, 0.05 μM, 0.2 μM, 1 μM, 10 μM, 20 μM, 30 μM and 40 μM and incubated for an additional 24 hrs. Two sets of plates were plated; one for cell counts and the other for RNA extraction.

b. Time Response

A total of 500, 000 cells/well were plated for the time point experiments in 6 well plates and incubated for 8, 24 and 48 hr time points. For the 72 hr time point, 250 000 cells were plated per well, to prevent overgrowth and nutrient exhaustion. After the 24 hr pre-incubation period, the 8,

24 and 48 hr time points were treated with 2 mL of media containing drug, whereas the 72 hr wells were given 3 mL of drug containing media. Controls were setup for all the time points where the cells were given media with no drug. Two sets of plates were plated; one for cell counts and the other for RNA extraction.

2.3 Determination of Dose and Time Response – Treatment with Paclitaxel

a. Dose Response

Cells were plated at a density of 500 000 cells/well in a 6 well plate and incubated at 37 ^{o}C with 5% CO_2. Following 24 hr, RNA was extracted from the 0 hr wells. Remaining culture wells were treated with 2 mL of media containing the following paclitaxel (TAX) concentrations: 0 μM, 0.001 μM, 0.005 μM, 0.01 μM, 0.05 μM, 0.2 μM, 1 μM, 10 μM, 20 μM, 30 μM and 40 μM and incubated for an additional 24 hr, following which RNA was extracted and analyzed.

b. Time Response

A total of 500, 000 cells/well were plated for the time point experiments in 6 well plates. After the 24 hr pre-incubation period, the cells were treated with 2 mL of media containing drug and incubated further for 24, 48 and 72 hr prior to RNA extraction and analysis.

2.4 Cell Counts

Following treatment, the medium was removed and floating cells were collected by centrifugation at 700 × g for 5 min. Attached cells were then collected (using 0.25% trypsin-EDTA) and both the floating and attached cells were counted using the Vi-CELL^{TM} XR Cell Viability Analyzer (Beckman Coulter Inc., Mississauga, Ontario). Cells were counted using the trypan blue dye exclusion method, where cells that remain transparent are counted as trypan blue excluding cells due to their intact membrane, while cells with damaged cell membrane are stained blue and counted as dead cells.

2.5 RNA Extraction and Analysis

Total RNA, including RNAs smaller that 200 nucleotides was purified using miRNeasy Mini Kit from Qiagen Laboratories (Mississauga, ON, Canada). Following treatment, the media was collected and added to a 15 mL conical. The tissue culture dish was then washed with PBS, which was also collected and added to the 15 mL conical tube and spun at 700 × g for 5 min to collect the floating cells. Following centrifugation, the supernatant was aspirated. To the cell culture dish containing attached cells, 700 µL of QIAzol lysis reagent was added, and the plates were scraped using a cell scraper to facilitate cell lysis. The lysis reagent collected from the plates was added to the cell pellet in the conical tube, where cells were further homogenized by passing the solution several times through a 20-gauge needle-fitted syringe (which will shear DNA) or vortexing when few cells were harvested until no cell clumps were visible. The homogenate was then transferred to 1.5 mL microfuge tubes and placed at room temperature for 5 mins, following which chloroform was added to the homogenate, and the tube was vortexed vigorously for 15 sec. The samples were then centrifuged for 15 min at 12000 × g at 4 ° C to allow phase separation to occur. The upper colorless aqueous phase consisting of RNA was carefully collected and added to a new collection tube consisting of 525 µL of anhydrous ethanol and vortexed. A total volume of 700 µL of sample was then loaded onto a RNeasy Mini spin column, and following manufacturer's instructions, RNA was eluted by adding 50 µL of RNase free water to the spin column twice. Quantity and integrity of isolated RNA was analyzed by capillary electrophoresis on Agilent RNA 6000 Nano chips obtained as part of Agilent 6000 Nano kits in the Agilent 2100 Bioanalyzer (Agilent Technologies Canada, Inc., Mississauga, ON, Canada).

2.6 Annexin-V Apoptosis Detection

To analyze the proportion of cells entering apoptosis, cells were stained with annexin-V and propidium iodide (PI) (CytoGLO-Annexin-V-FTIC Apoptosis Kit, IMGENEX, San Diego, CA, USA). Following treatment, both floating and adherent cells were collected into conical centrifuge tubes. Cells were pelleted at 700 × g for 5 min at room temperature (RT). After removal of the supernatant, PBS was added to wash the wells, which were centrifuged again at 700 × g for 5 min at RT. The supernatant was aspirated and the cell pellet was resuspended in 1 mL of media for counting using the Vi-CELL^{TM} XR Cell Viability Analyzer (Beckman Coulter Inc., Mississauga, Ontario). Following counting, 100 000 cells were aliquoted into 1 mL of cold PBS and pelleted by centrifuging at 300 × g for 5 min. After a second wash and pelleting, 100 µL of a proprietary binding buffer was then added to the cell pellet. The pellet was resuspended by flicking the tube and the cells were transferred to a flow tube. To stain the cells, 5µL of PI and 5 µL of annexin-V-FITC as provided by the manufacturer were added to the cells in the flow tubes and contents were mixed by swirling the tubes. The cells were incubated for 20 min at room temperature, in the dark, following which 400 µL of 1X binding buffer was added to the tube and analysis was performed using the BD FACSCanto II flow cytometer (Becton-Dickinson Biosciences, Mississauga, ON). 10000 events were analyzed for each sample using 525-nm band pass filter for annexin-V-FITC and 610-nm band pass filter for PI.

2.7 Cell Cycle Analysis

Floating and adherent cells were collected following treatment at several time points by trypsinization (with 0.25% trypsin-EDTA) and spun down at 700 × g for 5 min. The supernatant was aspirated and cell pellet was washed with 10 mL of cold PBS. The cells were spun at 700 × g for 5 min and the supernatant was discarded. The pellet was then resuspended in 1 mL of cold

PBS, to which 3 mL of cold 95% anhydrous ethanol was added. The fixed cells could be stored at -20 ° C until analysis. The fixed cells were spun at 700 × g for 5 min and the ethanol was removed, after which the cell pellet was washed with 10 mL of cold PBS for 5min at 700 × g. The PBS was aspirated, and 500 µL of stain solution (see below) was added to the cell pellet. Cells were incubated for 30 min at 37^{o} C before analyzing with the BD FACSCanto II flow cytometer (Becton-Dickinson Biosciences, Mississauga, ON) using a 610-nm band pass filter for PI. The stain solution (10 mL) was prepared using 0.1% sodium citrate, 0.3% NP-40, 100 mg/mL RNaseA, 100 µg/mL PI and 7.87 mL of water and was stored at 4 ° C in the dark.

2.8 Recovery Assay

Cells were plated in 0 µM, 0.005 µM and 0.2 µM DXL for 24, 48 and 72 hr in T75 flasks. A total of 5×10^{6} cells were plated for all conditions, except the 0 µM - 72 hr sample, for which 2.5×10^{6} cells were plated. Following the appropriate treatment time, cells were collected from each flask using 0.25% trypsin-EDTA and counted using the Vi-CELL^{TM} XR Cell Viability Analyzer (Beckman Coulter Inc., Mississauga, Ontario, CA). Based on the cell count (of trypan blue excluding cells) obtained, 500 000 cells were plated in 6 cm dishes in 6 mL of fresh media for counting following 24, 48, 72 and 96 hr of recovery. Cells were then counted at each of the time point to determine recovery of cells following drug treatment. This experiment was performed in triplicate.

2.9 DNA Laddering

Floating and adherent cells were collected following treatment at several time points by trypsinization (with 0.25% trypsin-EDTA) as described above. Genomic DNA was then isolated from each sample using the DNeasy Blood and Tissue Kit from Qiagen Laboratories (Mississauga, ON, CA) following manufacturer's instructions. The DNA concentration for each

sample was then determined using a NanoDrop ND-1000 spectrophotometer (Thermo Fisher Scientific Inc., Wilmington, DE, USA). Based on the concentrations obtained, 1 μg of DNA was added to 1X DNA gel loading dye (10X stock made using 3.9 mL glycerol, 500 μL of 10% (w/v) SDS, 200 μL EDTA (0.5 M), 0.025 g Bromophenol Blue). The samples were then loaded onto an 1.5% agarose gel containing ethidium bromide. Electrophoresis was then performed with TAE buffer and visualization was done under UV transillumination using ChemiDoc XRS system (Bio-Rad Laboratories, Mississauga, ON, CA).

2.10 Caspase-3 Activity Assay

To determine activation of caspase-3 a kit from Biovision, Caspase-3/CPP32 Colorimetric Assay Kit (BioVision Inc, Milpitas, CA, USA) was used. This kit measures the release of the chromophore p-nitroaniline (pNA) after cleavage from the labeled substrate DEVD-pNA by caspases that recognize DEVD sequence. The release of the chromophore is then quantified by absorption spectrophotometry.

To determine caspase-3 activity following treatment, cells were first plated in 6 cm dishes for 24, 48 and 72 hr and treated with 0 μM or 0.2 μM DXL. In all the untreated plates, 1×10^6 cells were plated to prevent overcrowding and nutrient deprivation, whereas 2.5×10^6 cells were plated for 0.2 μM DXL treated plates to ensure adequate cell numbers remained after treatment to allow for optimum protein harvest. Lysates were made by adding chilled Cell Lysis Buffer, provided in a Caspase-3/CPP32 Colorimetric Assay Kit (BioVision Inc, Milpitas, CA, USA), to the cell pellet. Protein concentration in lysates was determined using Pierce BCA Protein Assay Kit (Pierce, Rockford, IL, USA). Caspase-3 activity was then determined by following manufacturer's instructions for the assay kit. Absorbance readings were obtained using a PowerWave XS Microplate Spectrophotometer (BioTek Instruments Inc., Winooski, VT, USA).

The effect of a caspase-3 inhibition on caspase activity and on chemotherapy-dependent RNA disruption was determined by treating cells with and without the Caspase-3 Inhibitor Q-DEVD-Oph (10 μM) (BioVision Inc, Milpitas, CA, USA) at the time of treatment with docetaxel. At the treatment end point, cell lysates were prepared for monitoring caspase activity (as described above) and for assessing RNA quality on an Agilent 2100 Bioanalyzer (Agilent Technologies Canada, Inc., Mississauga, ON, CA) as described above.

2.11 Western Blot Analysis

Cell lysates for 0 μM – 24 hr and 0.2 μM DXL – 24, 48 and 72 hr were prepared from three biological replicate cultures using mammalian protein extraction reagent, M-PER (Thermo Scientific, Rockford, IL, USA) lysis buffer containing HALT protease inhibitor (Thermo Scientific, Rockford, IL, USA), sodium fluoride (50 mM), sodium orthovanadate (0.2 mM). After an appropriate treatment time, floating and adherent cells were collected using 0.25% trypsin-EDTA and washed 3 times in PBS before being harvested with lysis buffer. A volume of 100 μL of M-PER lysis buffer was added per 10 mg of cell pellet. To increase the protein concentration of lysates of the 72 hr samples treated with 0.2 μM docetaxel, 1/3 volume of lysis buffer was added. Protein concentration in the lysates was determined using the Pierce BCA Protein Assay Kit (Pierce, Rockford, IL, USA). A quantity of 20 μg of total protein in 6× sample buffer was heated at 100 ° C for 5 mins and resolved on 10% SDS-PAGE gels as described by Laemmli [90]. Proteins from the gel were transferred onto BioTrace PVDF membrane (Life Sciences, Pensacola, FL, USA). Following electrophoretic transfer, membranes were blocked with 5% milk solution in 1× TNE (obtained from a 20× TNE stock made using 100 mL of 1 M Tris-HCl (pH 7.5), 50 mL of 0.5 M EDTA (pH 8.0), 58.44 g of NaCl, H_2O to 500 mL) containing 0.1% Tween-20 (FisherBiotech, Thermo Fisher Scientific Inc., Waltham, MA, USA)

for 1 hour. Primary antibody was diluted in milk and incubated with the membrane on a rocker over night at 4 ° C. After washing the membrane for 3× 20 min in 1× TNE, the membrane was incubated with secondary antibody diluted in 5% milk for 1 hour at room temperature. Following treatment with the secondary antibody, membranes were washed for 3× 20 min in 1× TNE before the proteins were visualized using the enhanced chemiluminescence (ECL) method. The same membrane was reblotted with primary antibodies against Caspase-3 (3G2), PARP (46D11) and GAPDH (14C10) obtained from Cell Signaling Technology, Inc. (New England Biolabs, Ltd., Whitby, ON, CA) and β-Actin (C4) primary, obtained from Santa Cruz Biotechnology, Inc. (Santa Cruz, CA, USA). The goat anti-rabbit IgG-HRP and goat anti-mouse IgG-HRP secondary antibodies were obtained from Santa Cruz Biotechnology, Inc. (Santa Cruz, CA, USA). Separate gels were also prepared to be stained with 0.1 % Coomassie staining solution made using a PhastGel Blue R tablet (GE Healthcare Bio-Sciences AB, Uppsala, SE).

2.12 Statistical Analysis

The statistical significance of differences in values amongst samples was determined using a Student's t-test after application of the F-test to determine if the samples within an experiment contain significantly different amounts of variation. $p < 0.05$ was considered statistically significant.

3.0 Results

3.1 Dose Response

3.1.1 Cell Counts by Trypan Blue Staining

In order to assess the effect of docetaxel on A2780 cell proliferation, the number of cells present following treatment with increasing drug dose was counted using the Vi-CELL^{TM} XR Cell Viability Analyzer (Beckman Coulter Inc., Mississauga, Ontario). By using the trypan blue dye exclusion method, the number of total and trypan blue excluding cells (live/intact cells) following treatment was determined, and the number of live/intact cells present following treatment are reported in Figure 1. Since the cells were allowed an incubation period of 24 hr following plating, the number of trypan blue excluding cells was counted following this incubation period to ascertain the base level of cells present at the time of treatment (hereafter labelled 0 μM – 0 hr). The remaining values in Figure 1 are cell counts for drug treatments ranging from 0 to 40 μM docetaxel (DXL) for 24 hr. By comparing 0 μM – 0 hr and 0 μM – 24 hr samples, it is clear that the cells underwent at least one doubling time in 24 hr. The remaining drug treated sample values are compared to the 0 μM – 24 hr sample to determine if there is a significant difference in cell numbers in response to docetaxel treatment. Based on the bar graph in Figure 1, it is evident that there are significantly fewer number of cells in the treated samples, even at concentrations as low as 0.001 μM DXL ($p = 0.02$). The cell count seems to drop further until 0.005 μM DXL ($p = 2.31 \times 10^{-4}$), above which cell numbers appear to remain the same.

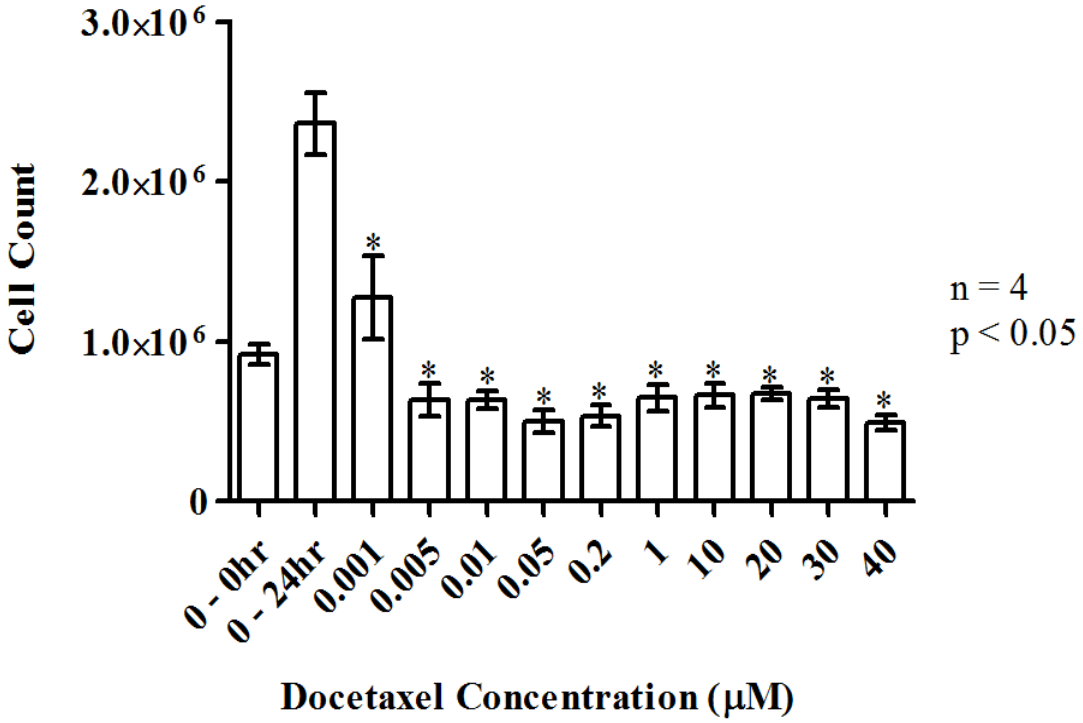

Figure 1. Changes in the cell count (trypan blue excluding) as a result of exposure to increasing concentrations of docetaxel. Each drug treated sample is compared to 0 μM – 24 hr control to determine if a significant difference exists.

3.1.2 Changes in RNA Concentration and RIN

Docetaxel-induced changes in RNA concentration and RIN following treatment were determined using capillary electrophoresis on an Agilent 2100 Bioanalyzer (Agilent Technologies Canada, Inc., Mississauga, ON, CA) and are shown in Figure 2. In Figure 2A, docetaxel-treated samples are compared to the 0 μM – 24 hr (control) sample to determine if significant changes in RNA concentration occur as a result of drug treatment. Compared to the control sample, a significant drop in RNA concentration is observed for the 0.01 μM ($p = 1.71 \times 10^{-2}$), 0.05 μM ($p = 5.32 \times 10^{-3}$), 0.2 μM ($p = 1.24 \times 10^{-2}$), 1 μM ($p = 4.68 \times 10^{-2}$), 10 μM ($p = 2.13 \times 10^{-2}$), 20 μM ($p = 7.43 \times 10^{-3}$), 30 μM ($p = 3.72 \times 10^{-3}$) and 40 μM ($p = 1.61 \times 10^{-3}$) docetaxel concentrations. However no significant change in RNA concentration is observed with the lower docetaxel concentrations of 0.001 μM ($p = 0.21$) and 0.005 μM ($p = 0.17$). There appears to be a trend of a drop in RNA concentration until 0.2 μM docetaxel, following which there seems to be an increase in RNA concentration, which decreases further with increasing drug concentration. Changes in the RIN value as a result of increasing docetaxel concentration are reported in Figure 2B. Although not statistically significant, there is a trend of decreasing RIN values with increasing dose at 0.001 μM ($p = 0.14$) until 0.2 μM ($p = 5.45 \times 10^{-2}$) docetaxel concentration is reached, following which, there appears to be a slight increase in RIN, similar to the observation made for RNA concentration. It is notable that with 0.2 μM docetaxel treatment a nadir in RNA concentration and RIN is observed. Although not as low as at the 0.2 μM docetaxel concentration, RIN values at some of the higher docetaxel concentrations do display a significant difference compared to the control: 20 μM ($p = 2.42 \times 10^{-2}$), 30 μM ($p = 3.84 \times 10^{-2}$) and 40 μM ($p = 8.63 \times 10^{-4}$).

A.

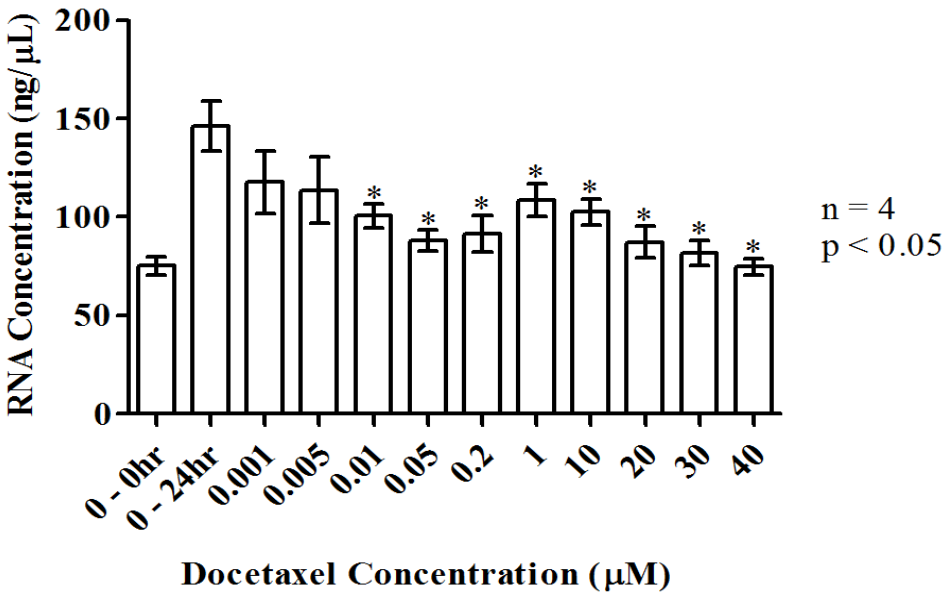

B.

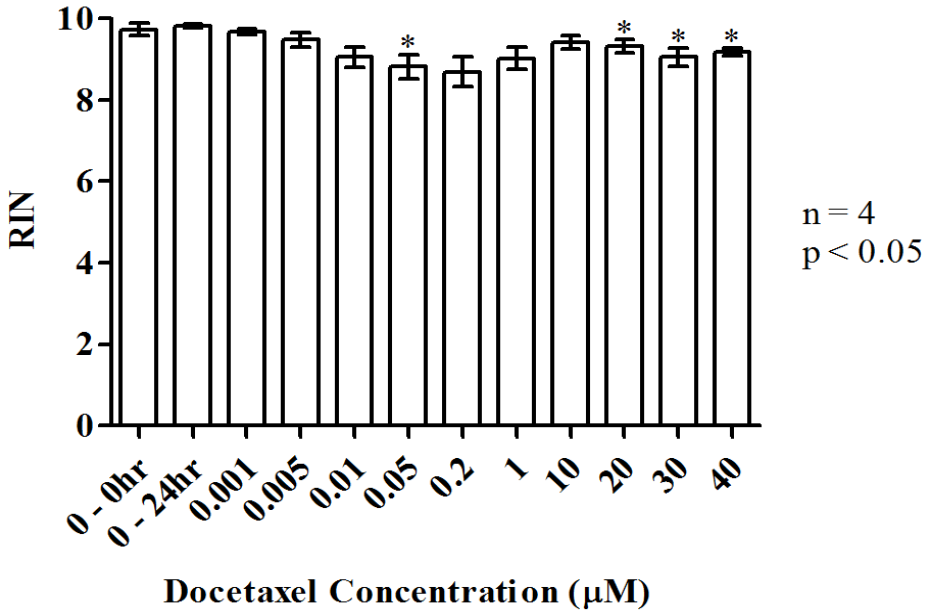

Figure 2. Changes in total RNA concentration (A) and RIN (B) as a result of varying docetaxel concentration. Significant difference between sample values was determined by comparing each of the drug treated samples to 0 µM – 24 hr control.

3.1.3 Changes in the Amount of RNA per Cell

Treatment with increasing concentrations of docetaxel resulted in changes in cell counts and RNA concentration; however, the concentrations of drug that resulted in a significant drop in cell count, did not result in a decrease in RNA concentration. Therefore, the amount of RNA per cell was calculated by dividing the amount of RNA isolated from the cell preparation by the total number of cells present following treatment for 24 hr with each drug concentration (Figure 3). Compared to the 0 μM – 24 hr control, there is a significant increase in the amount of RNA per cell as a result of treatment for all the drug concentrations being investigated: 0.001 μM ($p = 2.42 \times 10^{-2}$), 0.005 μM ($p = 8.22 \times 10^{-5}$), 0.01 μM ($p = 5.70 \times 10^{-5}$), 0.05 μM ($p = 1.45 \times 10^{-4}$), 0.2 μM ($p = 1.91 \times 10^{-4}$), 1 μM ($p = 3.88 \times 10^{-3}$), 10 μM ($p = 1.43 \times 10^{-3}$), 20 μM ($p = 1.58 \times 10^{-3}$), 30 μM ($p = 3.25 \times 10^{-3}$) and 40 μM ($p = 7.07 \times 10^{-4}$). The biggest change in RNA concentration per cell is observed for drug concentrations between 0.005 μM to 10 μM, following which, a drop in RNA per cell is observed.

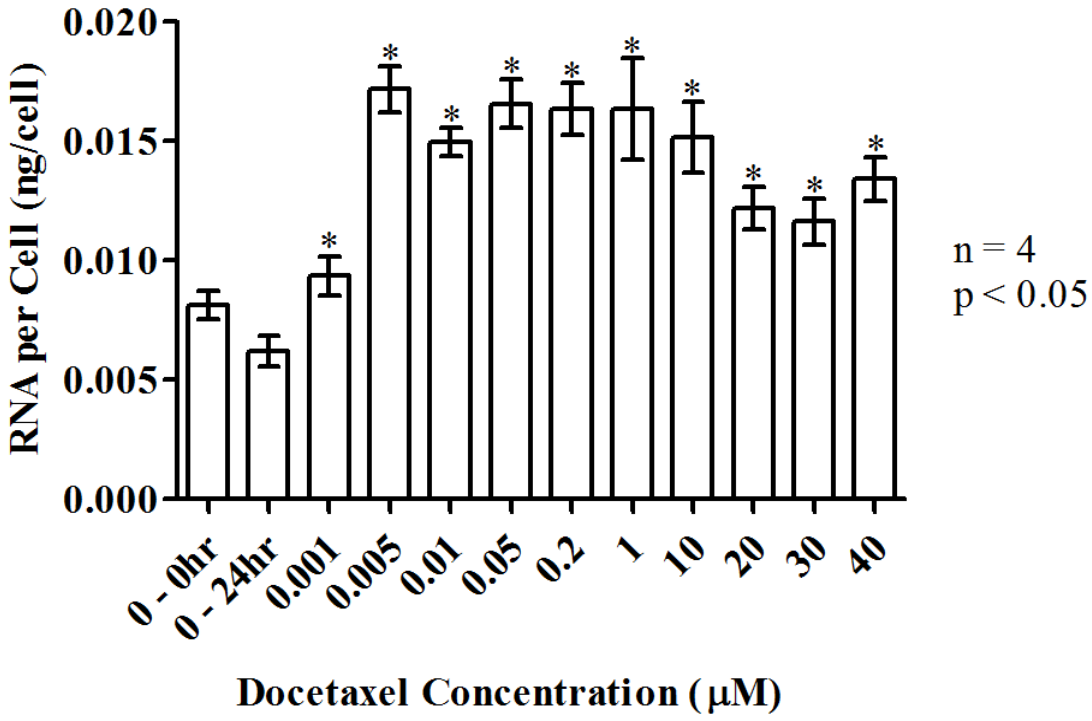

Figure 3. Dose dependent changes in the amount of RNA per cell. Each drug treated sample is compared to 0 – 24 hr control to determine significant difference.

3.1.4 Taxane-induced RNA Disruption

In order to determine if chemotherapy-dependent RNA disruption can be demonstrated *in vitro*, RNA preparations obtained from treated and untreated cells were analyzed using the Bioanalyzer and the resulting changes in rRNA pattern are shown in Figure 4 and 5. The electropherogram traces in Figure 4 show that all samples contained the 28S and 18S rRNA peaks; however, in some of the treated samples, unique peaks started to appear between the 28S and 18S, as well as below the 18S rRNA peaks. The average RNA concentrations as well as a representative value for RIN are also seen above each of the electropherogram traces in Figure 4a. Our findings show that RNA concentration and RIN started to decrease with increasing docetaxel concentration, however, starting at 1 μM DXL treatment, an increase in RNA concentration and RIN values was observed. Following the increase, a drop in these values is observed as a result of exposure to higher concentrations of drug. The electropherogram traces that result from the Bioanalyzer software program can also be visualized as gel-like image, which is shown in Figure 5. In the gel image, each peak observed in the electropherogram trace is intensified with respect to the other peaks within the samples, to better visualize the RNA quality, referred to as the individual scaling. In this type of depiction, we observed novel RNA bands (corresponding to the unique peaks within the electropherogram), which became evident at 0.005 μM docetaxel and were visible up to treatment with 30 μM docetaxel as seen in Figure 5a. These unique bands, thought to be degradation bands, were observed between 28S and 18S rRNA bands, as well as below the 18S rRNA band. Since these bands are apparent at a low docetaxel concentration of 0.005 μM, and appear to be strongest at the 0.2 μM docetaxel treatment, these concentrations were chosen to be studied further in subsequent experiments. Similar changes in RNA were observed as a result of treating A2780 cells with varying

paclitaxel concentrations (Figure 4b and 5b), demonstrating that the phenomenon of rRNA disruption can be applied to other taxanes.

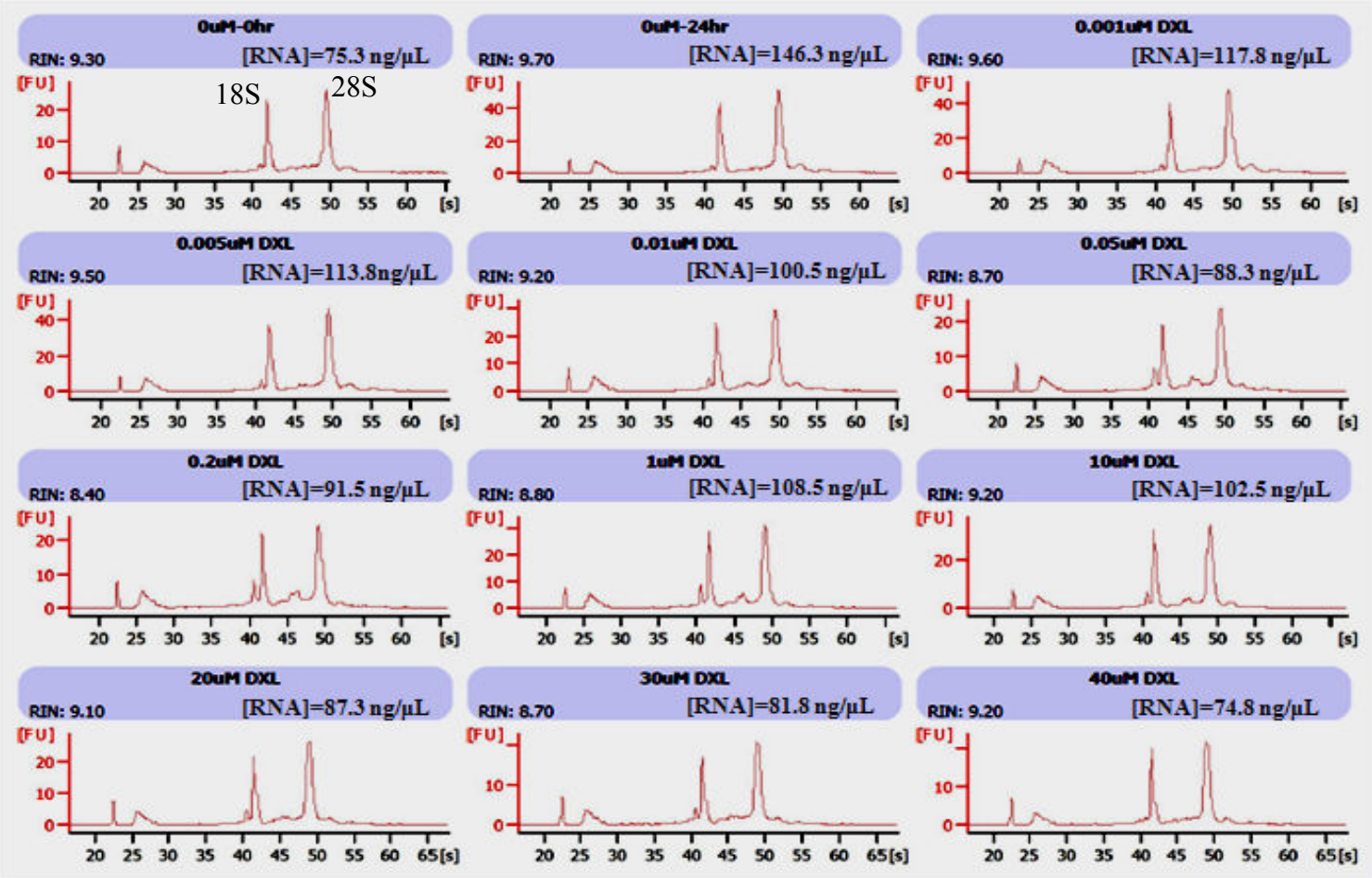

Figure 4a. Representative Bioanalyzer electropherogram traces of RNA of cells treated with 0 - 40 µM docetaxel for 24 hr. Note the induction of novel peaks between 28S and 18S rRNA, and below the 18S rRNA peaks in some of the drug treated samples.

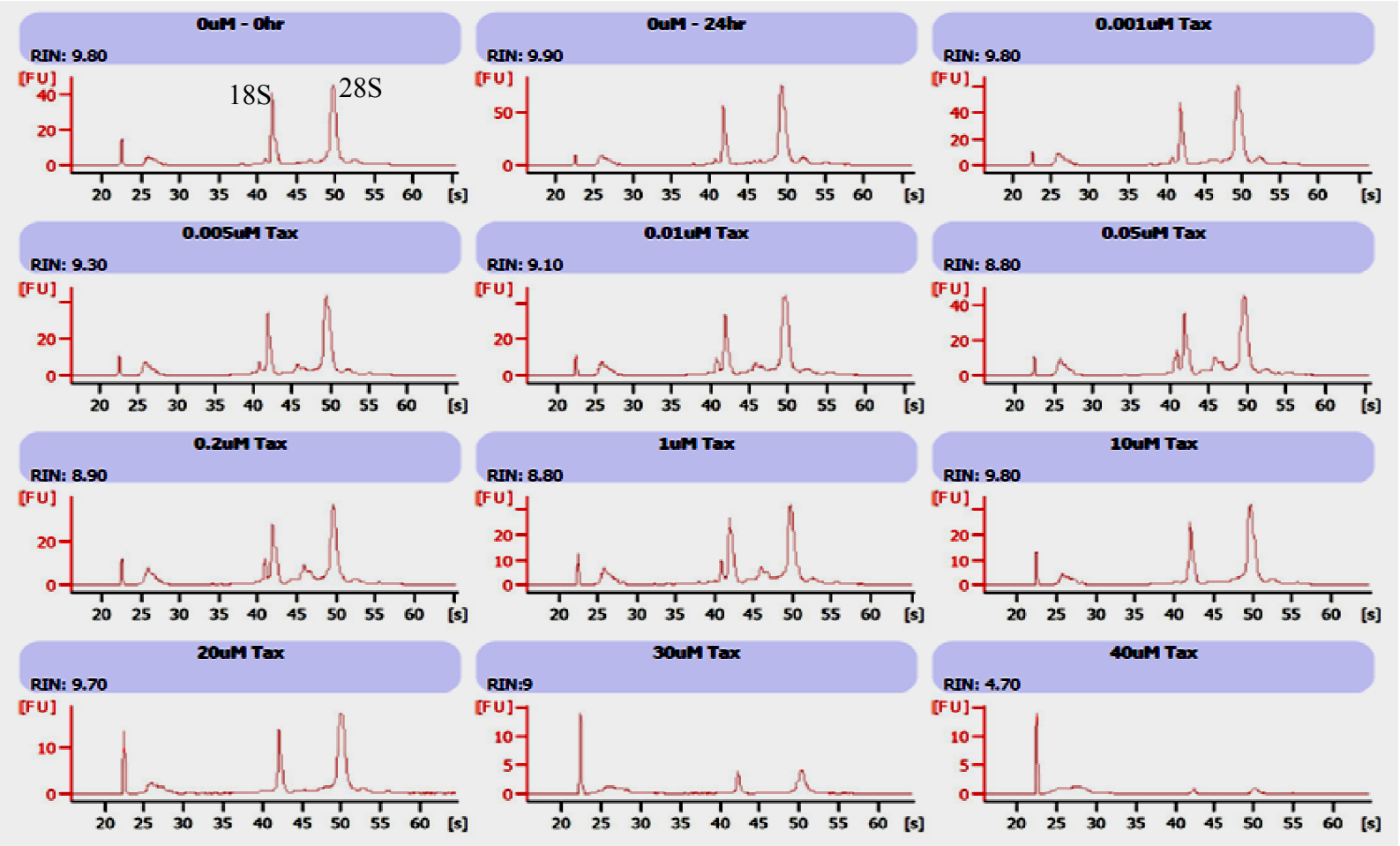

Figure 4b. Representative Bioanalyzer electropherogram traces of RNA of cells treated with 0 - 40 µM paclitaxel (Tax) for 24 hr. Note the induction of novel peaks between 28S and 18S rRNA, and below the 18S rRNA peaks in some of the drug treated samples. Shown are electropherogram traces, representative of six biological replicates.

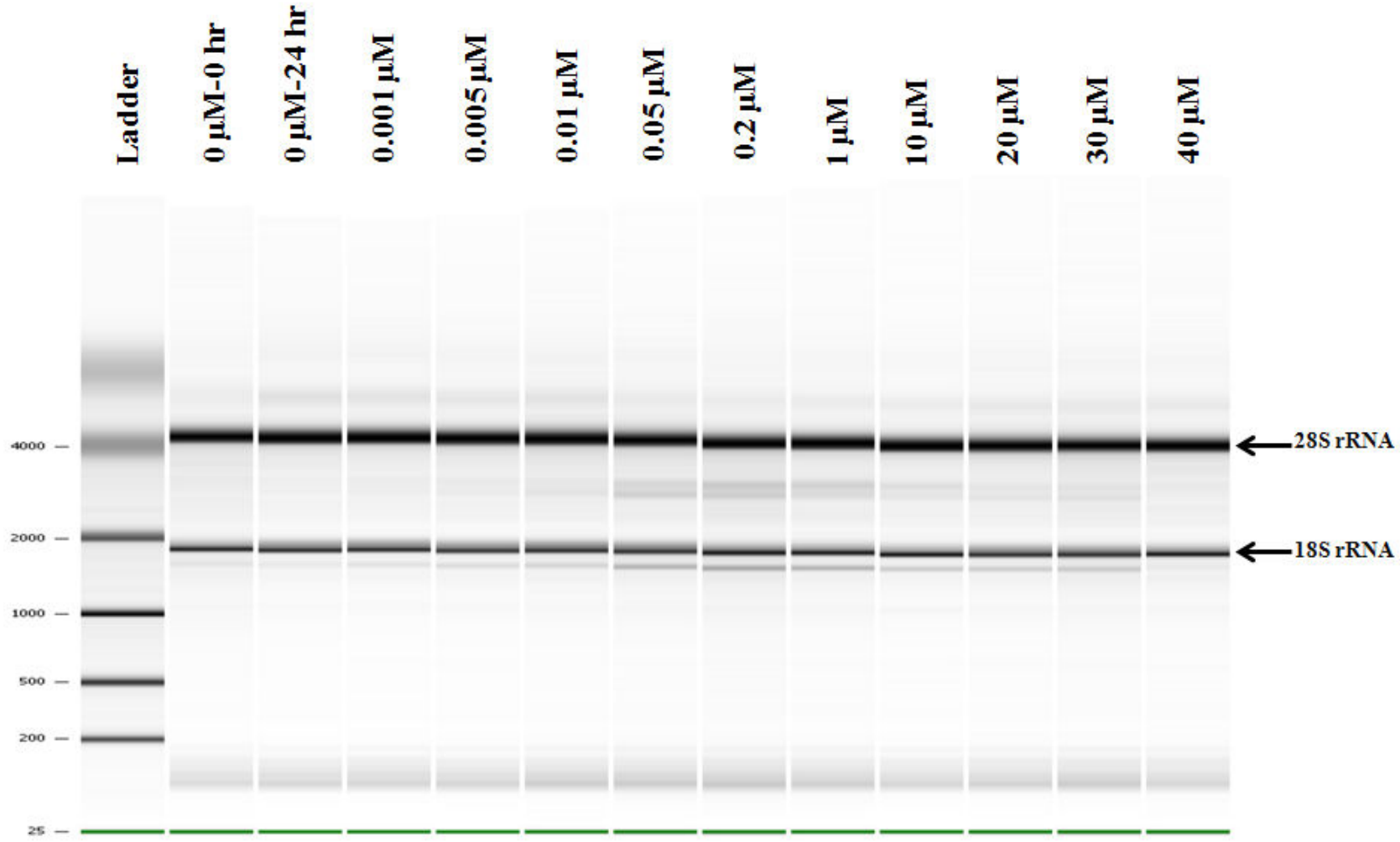

Figure 5a. A representative gel image (individual scaling) of the RNA quality of cells treated with 0 - 40 µM docetaxel for 24 hr. Note the appearance of unique bands between 28S and 18S rRNA, and below the 18S rRNA band.

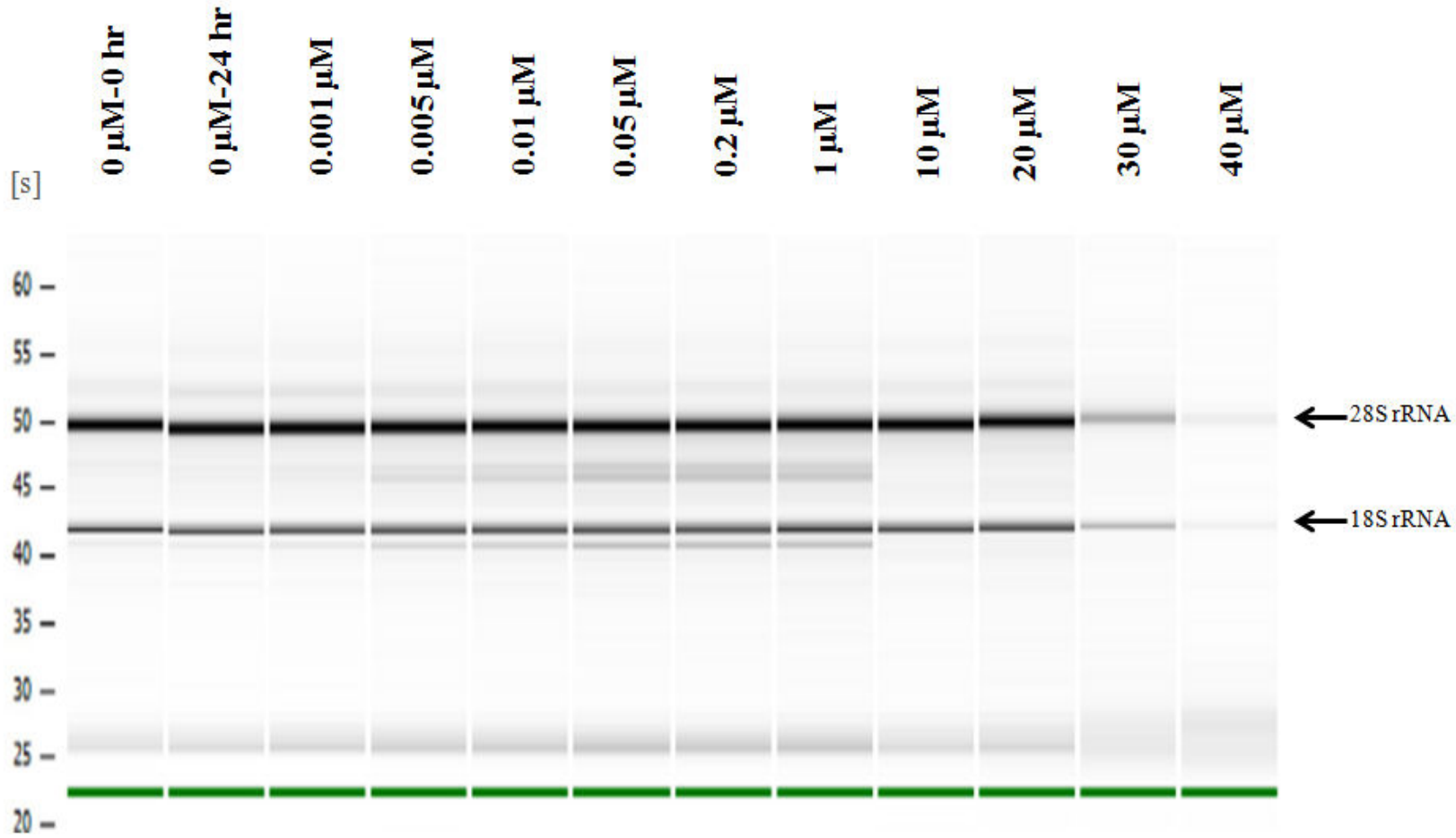

Figure 5b. Representative gel image (individual scaling) of RNA of cells treated with 0 - 40 µM paclitaxel (Tax) for 24 hr. Note the induction of novel bands between 28S and 18S rRNA, and below the 18S rRNA bands in some of the drug treated samples. Shown is a gel image, representative of six biological replicates.

3.2 Temporal Response

3.2.1 Cell Counts by Trypan Blue Staining

Similar to dose response, the changes in trypan blue excluding cells were determined as a result of treatment with 0.005 and 0.2 μM docetaxel for 8, 24, 48 and 72 hr of exposure. The resulting cell counts are shown in Figure 6. There was no significant difference observed for the different treatment conditions at the earlier time point of 8 hr [0.005 μM DXL ($p = 0.21$) and 0.2 μM DXL ($p = 5.71 \times 10^{-2}$)]. However, a significant drop in cell counts was observed for the docetaxel treated samples at 24 hr [0.005 μM DXL ($p = 3.84 \times 10^{-3}$) and 0.2 μM DXL ($p = 3.53 \times 10^{-4}$)], 48 hr [(0.005 μM DXL ($p = 8.43 \times 10^{-4}$) and 0.2 μM DXL ($p = 3.47 \times 10^{-6}$)] and 72 hr [(0.005 μM DXL ($p = 2.21 \times 10^{-5}$) and 0.2 μM DXL ($p = 1.57 \times 10^{-3}$)] of exposure when compared to 0 μM DXL samples in each time point.

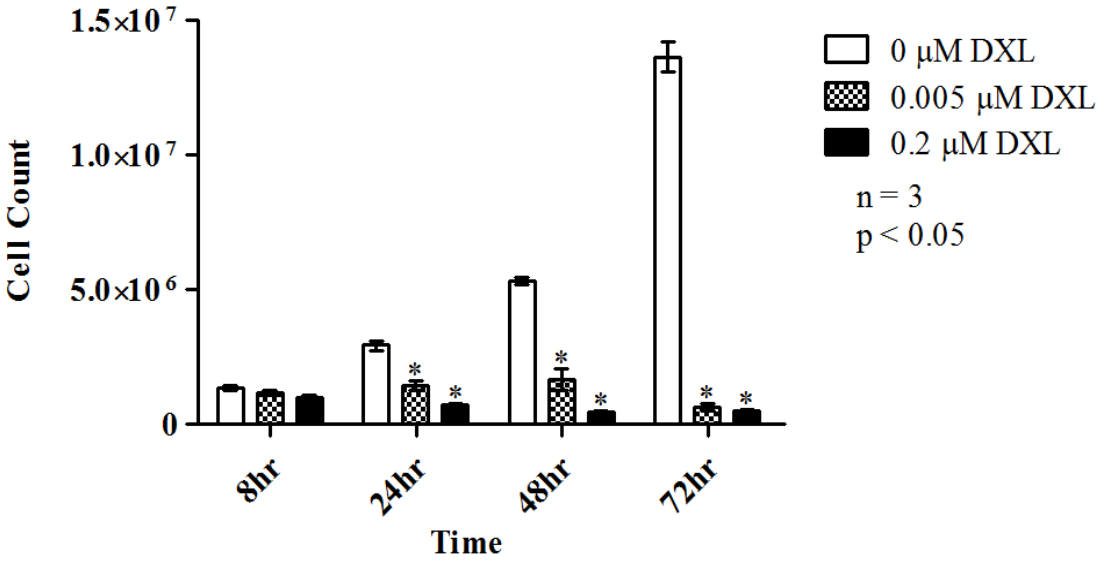

Figure 6. Effect of increasing docetaxel exposure time on trypan blue exclusion cell count for selected docetaxel concentrations. The drug treated samples within each time point are compared to the 0 µM DXL control to determine if a significant difference exists.

3.2.2 Changes in RNA Concentration and RIN

Changes in RNA concentration and RIN were measured as a result of increasing exposure times, and are reported in Figure 7. No significant changes in RNA concentration were observed at 8 hr [0.005 μM ($p = 0.71$) and 0.2 μM ($p = 0.84$)] or 24 hr [0.005 μM ($p = 0.46$) and 0.2 μM ($p = 0.10$)] of exposure as shown in Figure 7A. A significant decrease in RNA concentration was observed at 48 and 72 hr for 0.2 μM DXL ($p = 3.56 \times 10^{-2}$ and $p = 2.49 \times 10^{-3}$ respectively), however, for 0.005 μM treatment, a significant difference in RNA concentration is observed only at 72 hr of exposure ($p = 3.00 \times 10^{-3}$). In terms of RIN values, no significant changes are observed at 8 hr of exposure for the two drug concentrations being investigated [0.005 μM DXL ($p = 0.49$) and 0.2 μM DXL ($p = 0.72$)], as shown in Figure 7B. A distinct and significant drop in RNA integrity is observed for the 0.2 μM treated sample starting at 24 hr ($p = 6.07 \times 10^{-4}$), however, RIN values declined significantly in both the docetaxel treated samples at 48 hr [0.005 μM DXL ($p = 7.00 \times 10^{-4}$) and 0.2 μM DXL ($p = 4.47 \times 10^{-7}$)] and 72 hr [0.005 μM DXL ($p = 2.71 \times 10^{-8}$) and 0.2 μM DXL ($p = 1.04 \times 10^{-4}$)]. In the 0 μM control sample, the RIN value remains high at all the treatment time points.

A.

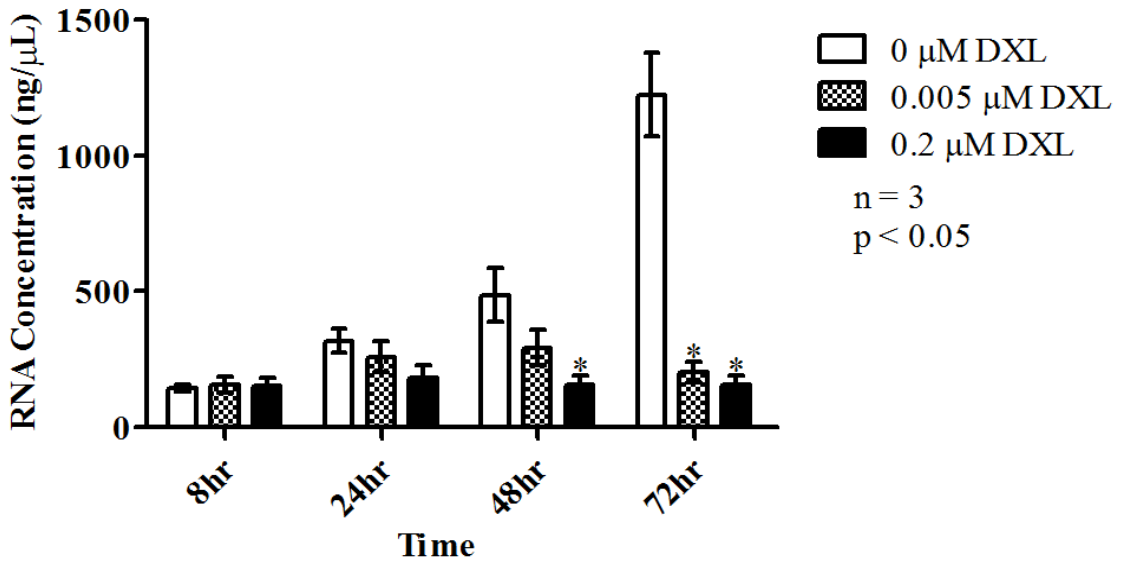

B.

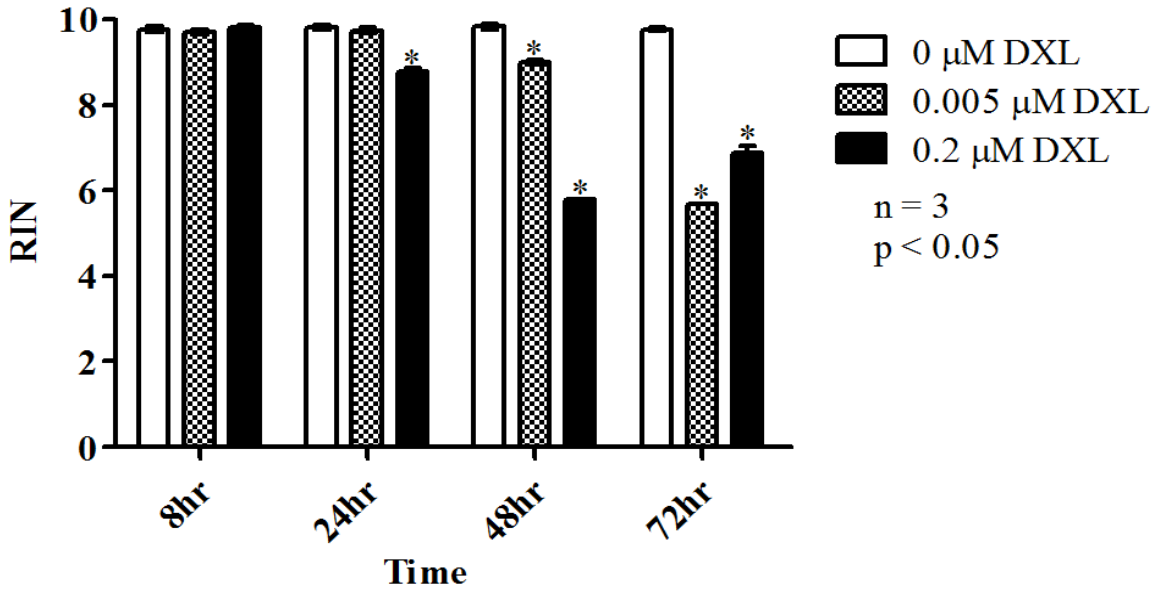

Figure 7. Changes in RNA concentration (A) and RIN (B) as a result of increasing docetaxel exposure time for selected drug concentrations. Significant difference between values is determined by comparing the drug treated sample at each time point to 0 μM DXL control.

3.2.3 Changes in the Amount of RNA per Cell

Since an increase in the amount of RNA per cell was observed as a result of increasing dose, changes in the amount of RNA per cell were also determined for the temporal response. As shown in Figure 8, a significant increase in the amount of RNA per cell was observed for the 0.2 μM docetaxel treated samples at 24 hr ($p = 4.67 \times 10^{-2}$), 48 hr ($p = 1.17 \times 10^{-2}$) and 72 hr ($p = 5.55 \times 10^{-3}$) exposure. However, for the 0.005 μM treatment sample, a significant increase compared to the control (0 μM) was observed only for the 72 hr exposure ($p = 3.84 \times 10^{-2}$). Although not significantly higher, a trend of increasing RNA per cell is observed for the 0.005 μM treated sample at 24 ($p = 0.13$) and 48 hr ($p = 0.06$). The amount of RNA per cell does not seem to be changing for the 0 μM treated samples across all the time points. No significant changes were observed for RNA per cell at the 8 hr time point for any treatment conditions [0.005 μM DXL ($p = 0.46$) and 0.2 μM DXL ($p = 0.34$)].

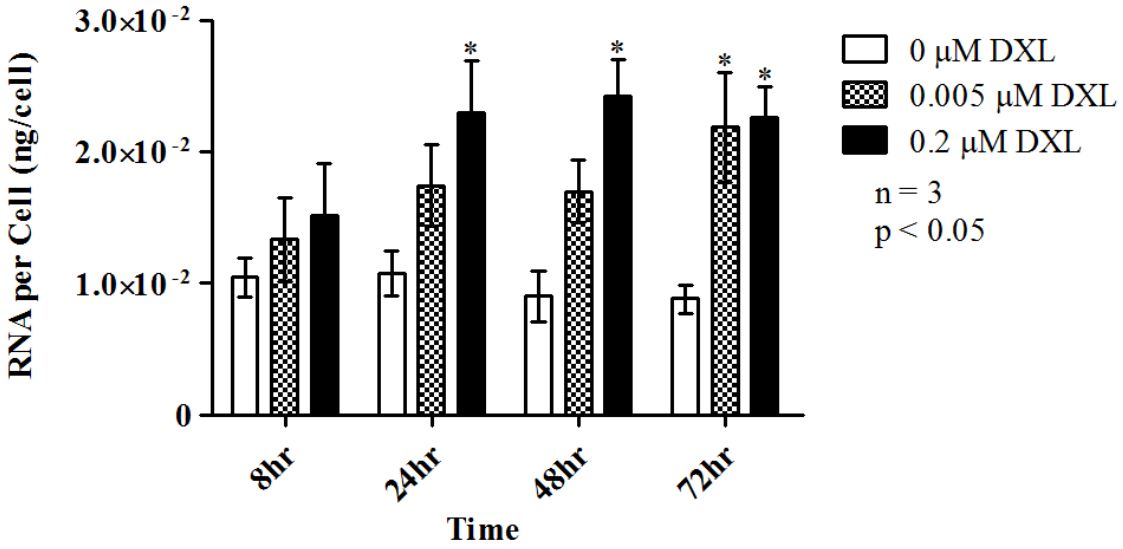

Figure 8**.** Changes in the amount of RNA per cell as a result of increasing length of exposure to docetaxel. Significant difference between values was determined by comparing the treated samples to 0 μM DXL control at each time point.

3.2.4 Taxane-induced rRNA Disruption

The time dependence of docetaxel-induced rRNA disruption in A2780 cells is shown in Figure 9a and Figure 10a. The electropherogram traces as well as the gel image show no disruption products at the earlier time point (8 hr), and that the abnormal peaks (and corresponding bands in the gel image) are evident at 24 hr of drug exposure, showing up clearly in the 0.2 μM treated sample. By increasing the treatment time to 48 hr, the electropherogram trace for the 0.2 μM docetaxel treated sample, clearly demonstrates that the sizes of the intact 18S and 28S rRNA peaks are decreasing, whereas the novel, unique peaks are increasing in intensity. This is particularly noticeable in the gel image (individual scaling) as shown in Figure 10a for the 0.2 μM DXL sample at 72 hr exposure, where the intensity of the 28S and 18S bands is becoming weak, while the unique bands increase in intensity. Comparable changes are observed as a result of paclitaxel treatment, where treatment with 1 μM TAX results in a time-dependent increase in rRNA disruption (Figure 9b and Figure 10b), with paclitaxel treatment resulting in two aberrant bands below the 18S rRNA band, whereas treating A2780 cells with docetaxel resulted in only one unique band below the 18S rRNA.

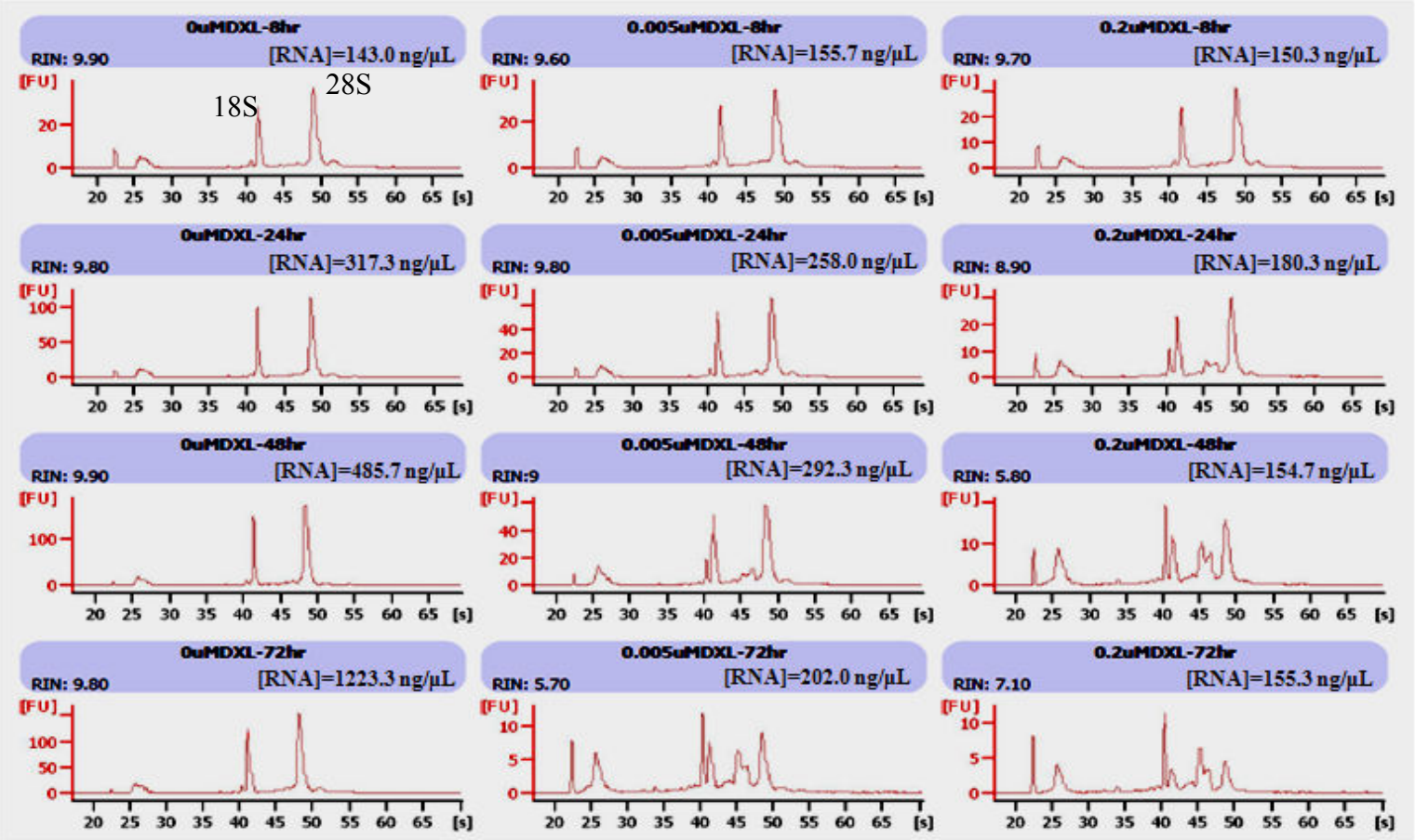

Figure 9a**.** Representative electropherogram traces of RNA of cells treated for 8, 24, 48 and 72 hr with 0.005 and 0.2 µM docetaxel. Note the presence and increase in the intensity of the novel peaks between 28S and 18S rRNA, as well as below 18S rRNA, as a result of increasing exposure time.

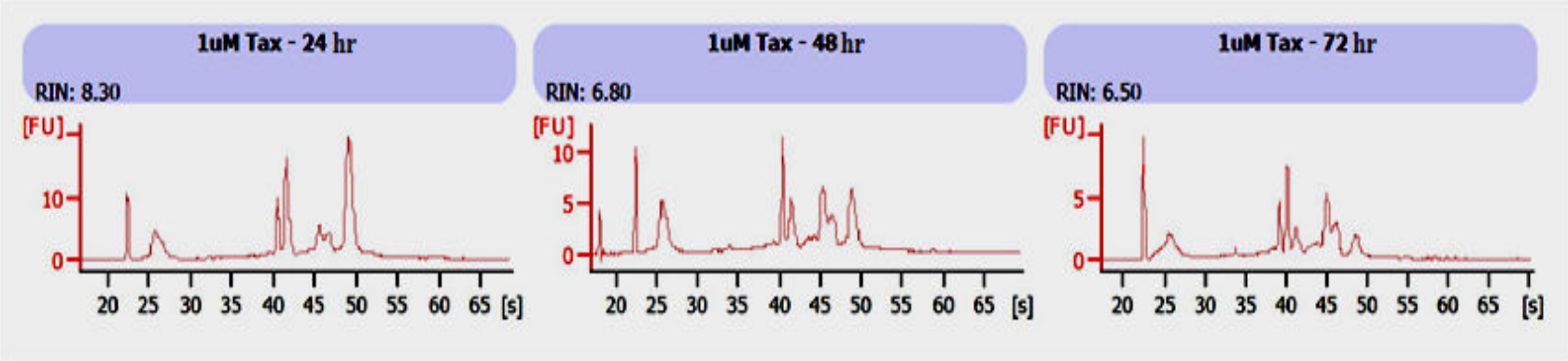

Figure 9b. Representative electropherogram traces of RNA of cells treated for 24, 48 and 72 hr with 1 μM paclitaxel. Note the presence and increase in the intensity of the novel peaks between 28S and 18S rRNA, as well as below 18S rRNA, as a result of increasing exposure time. Shown are representative electropherogram traces from three biological replicates.

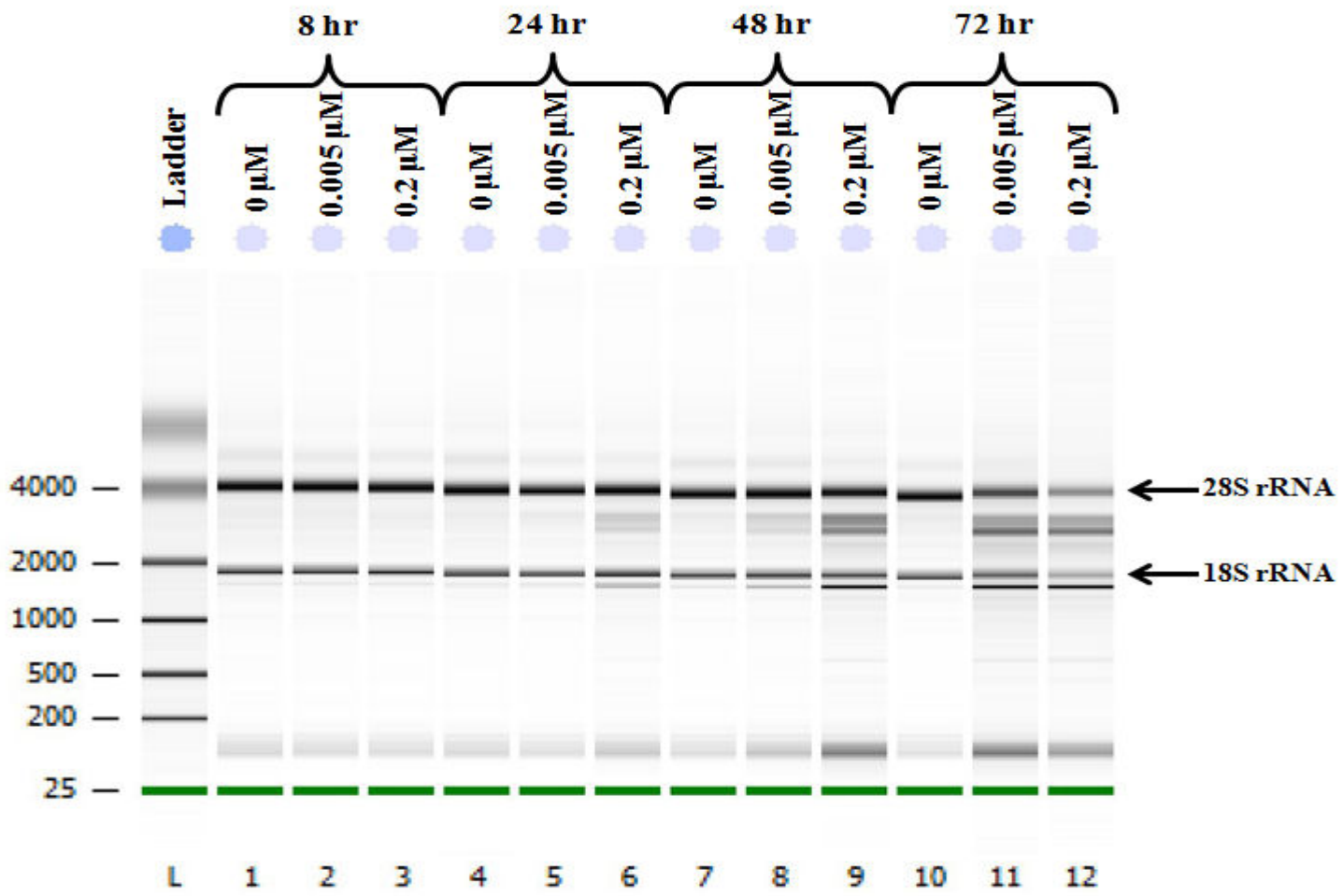

Figure 10a. Temporal changes in rRNA pattern across 8, 24, 48 and 72 hr of exposure to 0.005 and 0.2 µM docetaxel. Note the presence and increase in the intensity of the unique bands between 28S and 18S rRNA, as well as below 18S rRNA, as a result of increasing exposure time in the gel image (individual scaling).

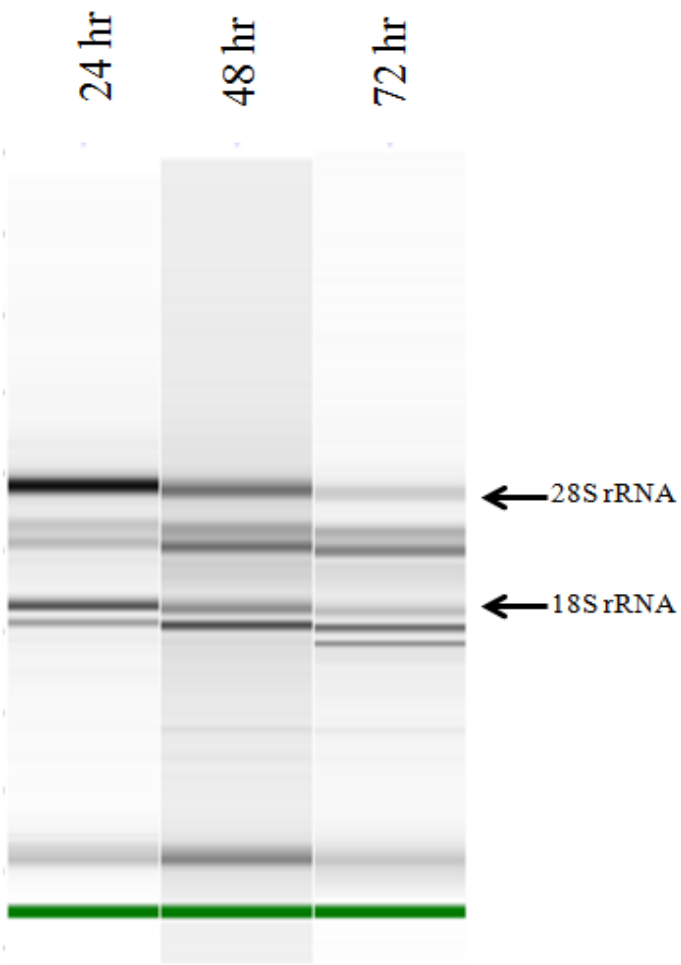

Figure 10b. Temporal changes in rRNA pattern across 24, 48 and 72 hr of exposure to 1 μM paclitaxel. Note the presence and increase in the intensity of the unique bands between 28S and 18S rRNA, as well as below 18S rRNA, as a result of increasing exposure time in the gel image (individual scaling). Shown are representative image from three biological replicates.

3.3 Cell Cycle Analysis

The effect of docetaxel treatment on the cell cycle (n = 3) was investigated using propidium iodide staining of cells following treatment with 0.2 μM docetaxel for 8, 24, 48 and 72 hr and is shown in Figure 11. The binding of propidium iodide to DNA produces a fluorescence value which reflects the DNA content within fixed cells. In the graphs, the fluorescence peak labelled G1 corresponds to cells containing a diploid (2n) amount of DNA. Cells in G2/M phase contain a 4n amount of DNA, and thus have an increased fluorescence, whereas cells in S phase are undergoing DNA replication, and have intermediate fluorescence values between that of the G1 and G2/M phase. The sub G1 peak represents cells containing a hypodiploid amount of DNA, and is often associated with apoptotic bodies. The untreated samples for each of the time points in Figure 11A show very little change in their fluorescence peaks, indicating no change in the cell cycle. The DNA profiles of untreated samples at 48 and 72 hr show a decrease in the number of cells in the G2/M phase, indicating diminished cell cycle progression, possibly due to gradual nutrient exhaustion. Comparing the untreated cells to 0.2 μM docetaxel treated samples in Figure 11B, it is evident that the population of cells undergoing treatment have an altered DNA content. After 8 hr in 0.2 μM docetaxel, cells appear to be accumulating in the G2/M phase of the cell cycle and there is a reduction in the size of the G1 peak when compared to the untreated sample at this time point. By 24 hr, there is no discernible G1 peak and an extensive population of cells are accumulating in the G2/M phase. At 48 hr, there are very few cells undergoing normal cell cycle progression, with the majority of the population containing less than 2n amount of DNA, detected as the sub G1 peak. At the 72 hr time point, almost all of the population contains very little DNA, with the sub G1 peak being the

only identifiable peak, indicating the presence of apoptotic bodies containing degraded or fragmented DNA.

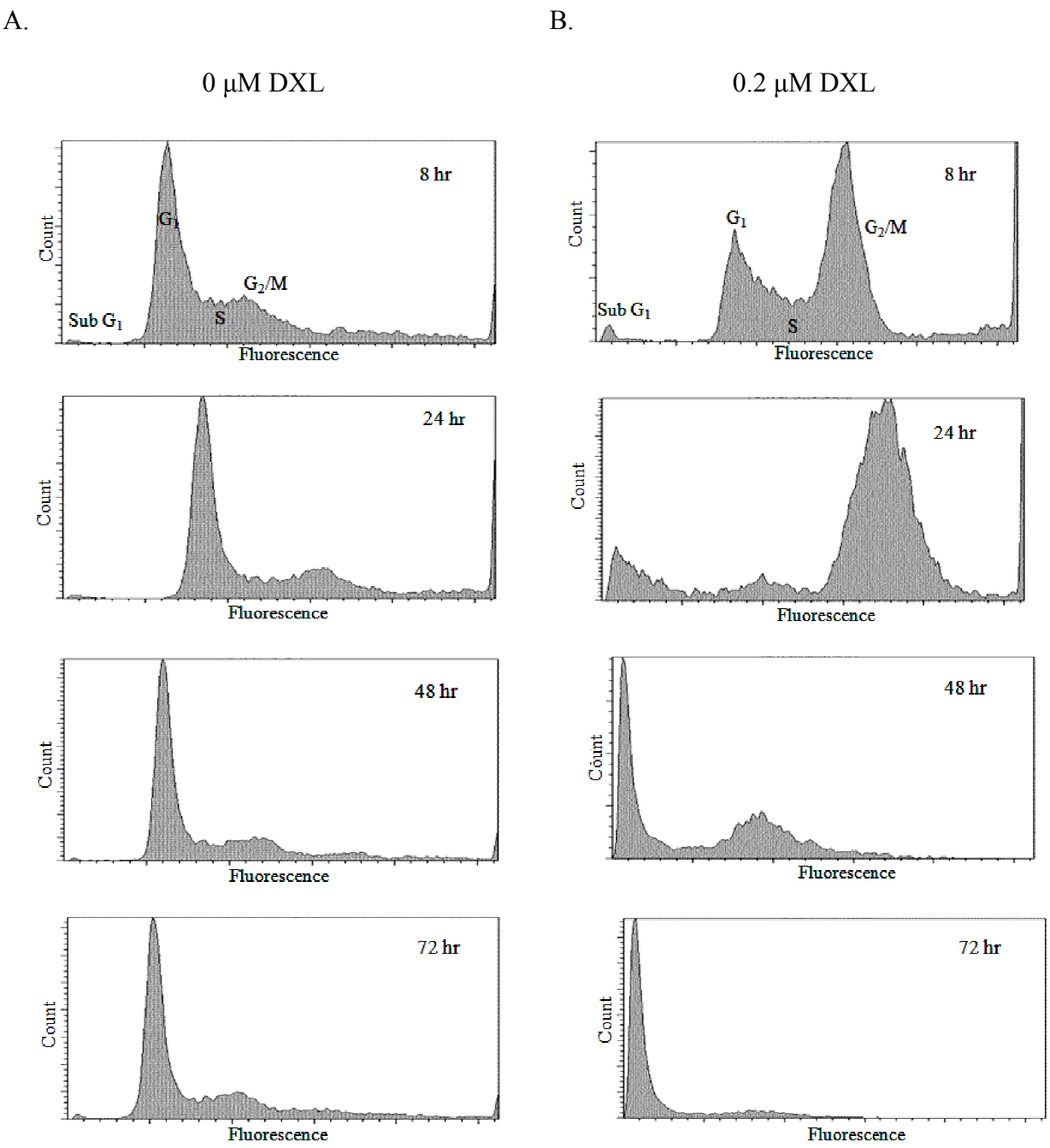

Figure 11. The effect of 0.2 µM docetaxel treatment on cell cycle progression and DNA quality across 8, 24, 48 and 72 hr exposure.

3.4 Apoptosis Detection Using Annexin-V and Propidium Iodide Staining

Staining of A2780 cells treated with docetaxel using annexin-V and propidium iodide (PI) was used to determine if apoptosis induction occurred as a result of treatment. Cells were treated with either 0 or 0.2 μM of docetaxel for 8, 24, 48 and 72 hr, following which they were collected and stained with annexin-V-FITC and PI and analyzed using flow cytometry. The experiment was performed in triplicate. The results from this assay are shown in Figure 12, where each scatter plot contains four quadrants. Quadrant 1 (Q1) contains cells with PI staining only, indicative of necrosis, quadrant 2 (Q2) contains cells stained with both annexin-V and PI, which are representative of cells in late apoptosis, quadrant 3 (Q3) are unstained, healthy cells and quadrant 4 (Q4) contains annexin-V positive, PI negative cells which represent early apoptotic cells. The numbers located in the upper right corner of quadrants 1, 2 and 4, and bottom left for quadrant3, indicate the percentage of cells in each quadrant, with the standard deviation in parenthesis. To determine if there was a significant difference, the percentage of cells in each quadrant in the treated sample was compared to that of the untreated cells in each corresponding quadrant. At 8 hr, no significant difference exists for any of the quadrants except for Q4, where a slight (but significant) decrease in annexin-V positive cells was observed as a result of DXL treatment [Q1 ($p = 0.10$), Q2 ($p = 0.87$), Q3 ($p = 0.38$) and Q4 ($p = 2.54 \times 10^{-2}$)]. At 24 hr, a significant difference between the 0 μM and 0.2 μM treated sample is noted for all quadrants [Q1 ($p = 1.51 \times 10^{-4}$), Q2 ($p = 1.35 \times 10^{-3}$), Q3 ($p = 1.03 \times 10^{-5}$), Q4 ($p = 4.81 \times 10^{-6}$)], however, it is apparent that there is a much greater increase in the number of early apoptotic cells (Q4) with treatment at this time point. The percentage of early apoptotic cells increases further by 48 hr ($p = 9.98 \times 10^{-9}$), and remains significantly higher at 72 hr ($p = 1.84 \times 10^{-7}$) of exposure.

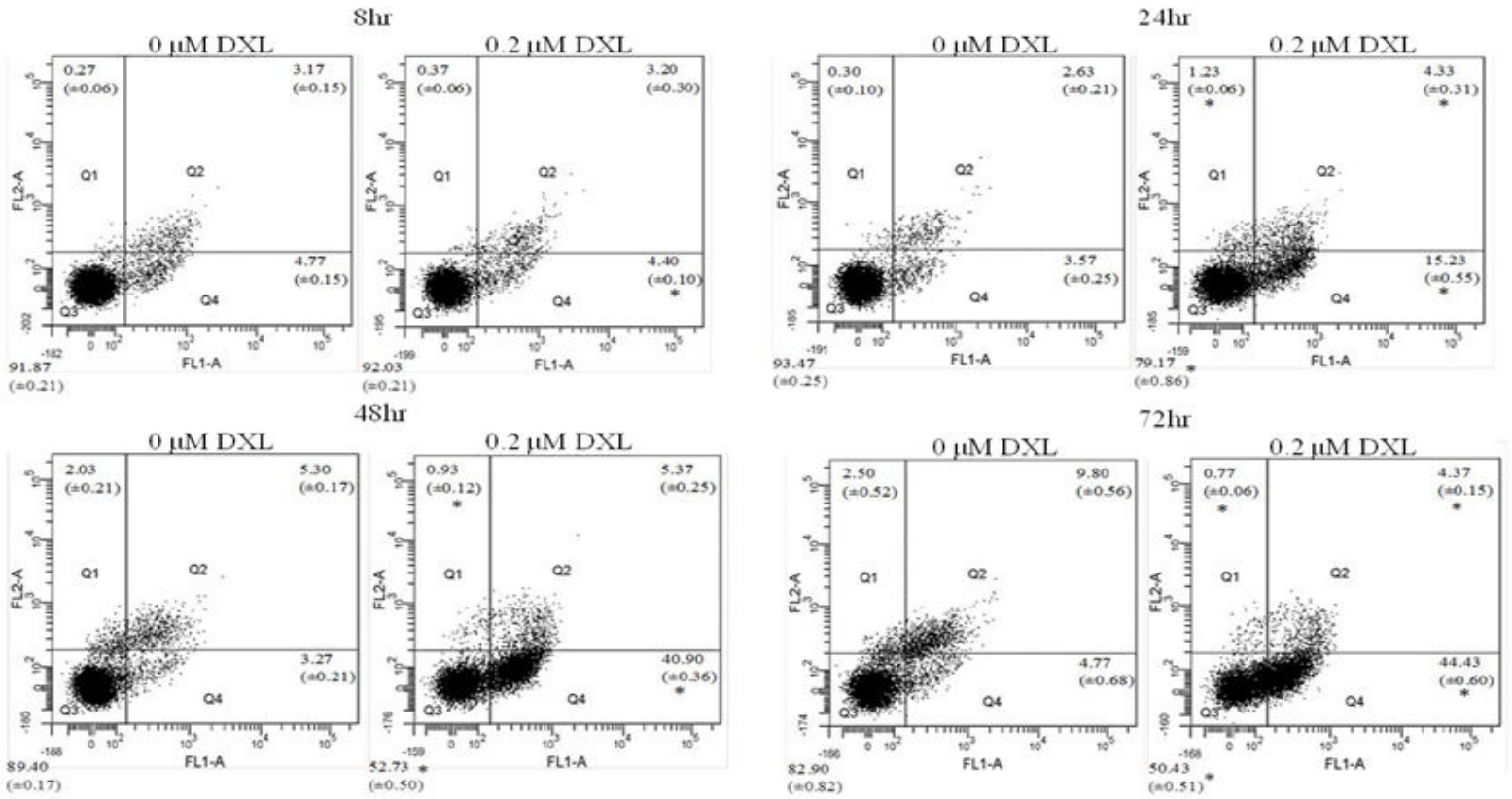

Figure 12. A2780 cells untreated and treated with 0.2 µM DXL for 8, 24, 48 and 72 hr, stained using annexin-V- FITC and propidium iodide. A time dependent increase in early apoptotic cells with treatment is observed. Quadrant 1 (Q1) = Necrotic cells; Quadrant 2 (Q2) = Late apoptotic cells; Quadrant 3 (Q3) = Healthy cells; Quadrant 4 (Q4) = Early apoptotic cells. The numbers indicate percentage of events identified in each quadrant, with the standard deviation below in parenthesis. An asterisk denotes significant difference ($p < 0.05$) between the corresponding quadrants in the untreated and treated samples.

3.5 Recovery Assay

Although there was an increase in the percentage of early apoptotic cells observed as a result of drug treatment, there was no significant increase in the number of dead cells, whether from necrosis or apoptosis (Figure 12). In order to determine if cells treated with docetaxel are able to recover and proliferate upon drug removal, cells were collected following treatment with 0.005 and 0.2 μM of docetaxel for 24, 48 and 72 hr, and re-plated in fresh media. The proliferative capacity of the cells was determined by counting cells every twenty four hours until 96 hr to determine the number of trypan blue excluding cells present. The results from this assay are shown in Figure 13. When cells were treated for 24 hr with 0.005 μM docetaxel, they are able to recover and proliferate, albeit, at a much slower rate (either due to delay in resumption of active cell proliferation or due to a slower growth rate) compared to 0 μM as shown in Figure 13A. The cells treated with 0.2 μM docetaxel for 24 hr are unable to recover and show no evidence of proliferation. Similar results are found following treatment for 48 hr as shown in Figure 13B, although, the cells treated with 0.005 μM docetaxel are recovering at a slower rate compared to those treated for 24 hr. As shown in Figure 13C, it is evident that cells that have undergone 0.005 and 0.2 μM docetaxel treatment for 72 hr are unable to recover or proliferate. Since rRNA disruption is observed to be the strongest at 72 hr of treatment for both 0.005 and 0.2 μM docetaxel, and an increase in the early apoptotic population is observed for the higher drug concentration at 24, 48 and 72 hr (Figure 12), these results suggest that cells showing strong RNA disruption are beginning to undergo apoptosis but are unable to recover and proliferate.

A.

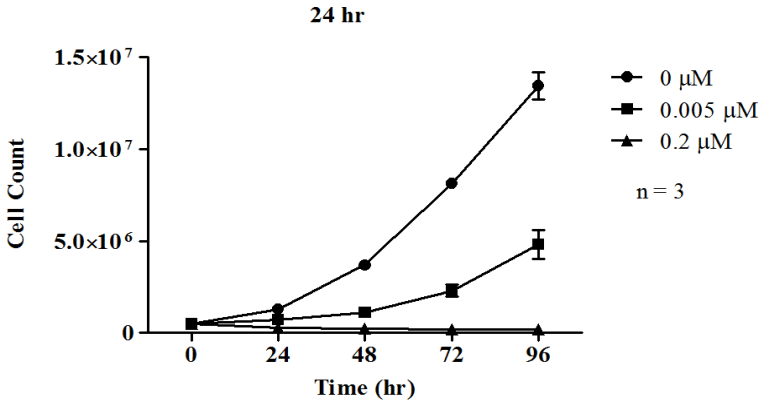

B.

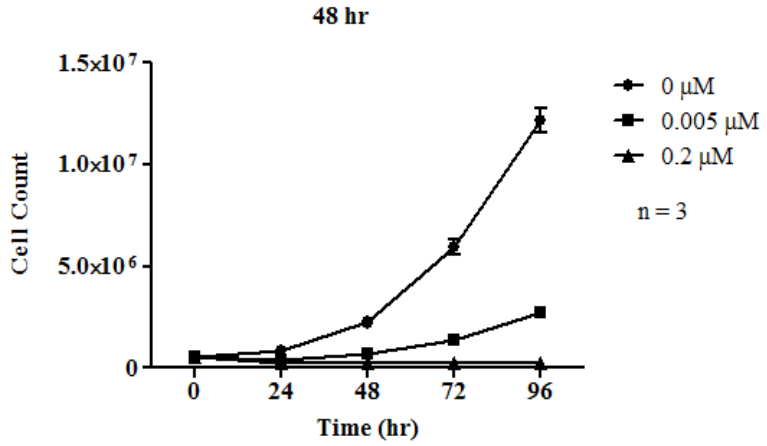

C.

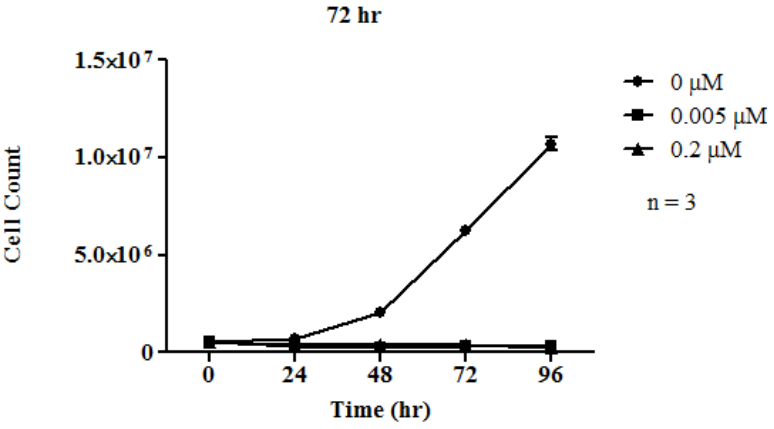

Figure 13. Recovery and proliferative capabilities of A2780 cells treated for 24, 48 and 72 hr with 0.005 and 0.2 µM docetaxel.

3.6 DNA Laddering

The results from the recovery assay suggest that at the higher drug dose of 0.2 μM docetaxel, strong rRNA disruption is observed and the cells are unable to recover and proliferate. To assess if cells are undergoing apoptosis, DNA laddering was assayed (Figure 14). DNA was extracted from cells treated with 0 and 0.2 μM docetaxel at several time points. Interestingly, A2780 cells treated with docetaxel do not show DNA laddering, even at the later time points where extensive RNA disruption is observed and cells are unable to recover. Some samples show a denser DNA band compared to the others (0 μM – 48, 72 hr and 0.2 μM – 24 hr), possibly due to an excess amount of DNA loaded. Although not the typical oligonucelosomal laddering, a smear of DNA fragments, with some visible bands towards the bottom of the lane, are observed for the positive controls, Jurkat cells treated with 5 μM and 30 μM Etoposide, indicating DNA damage and fragmentation. However, a similar pattern was not observed for any of the A2780 samples.

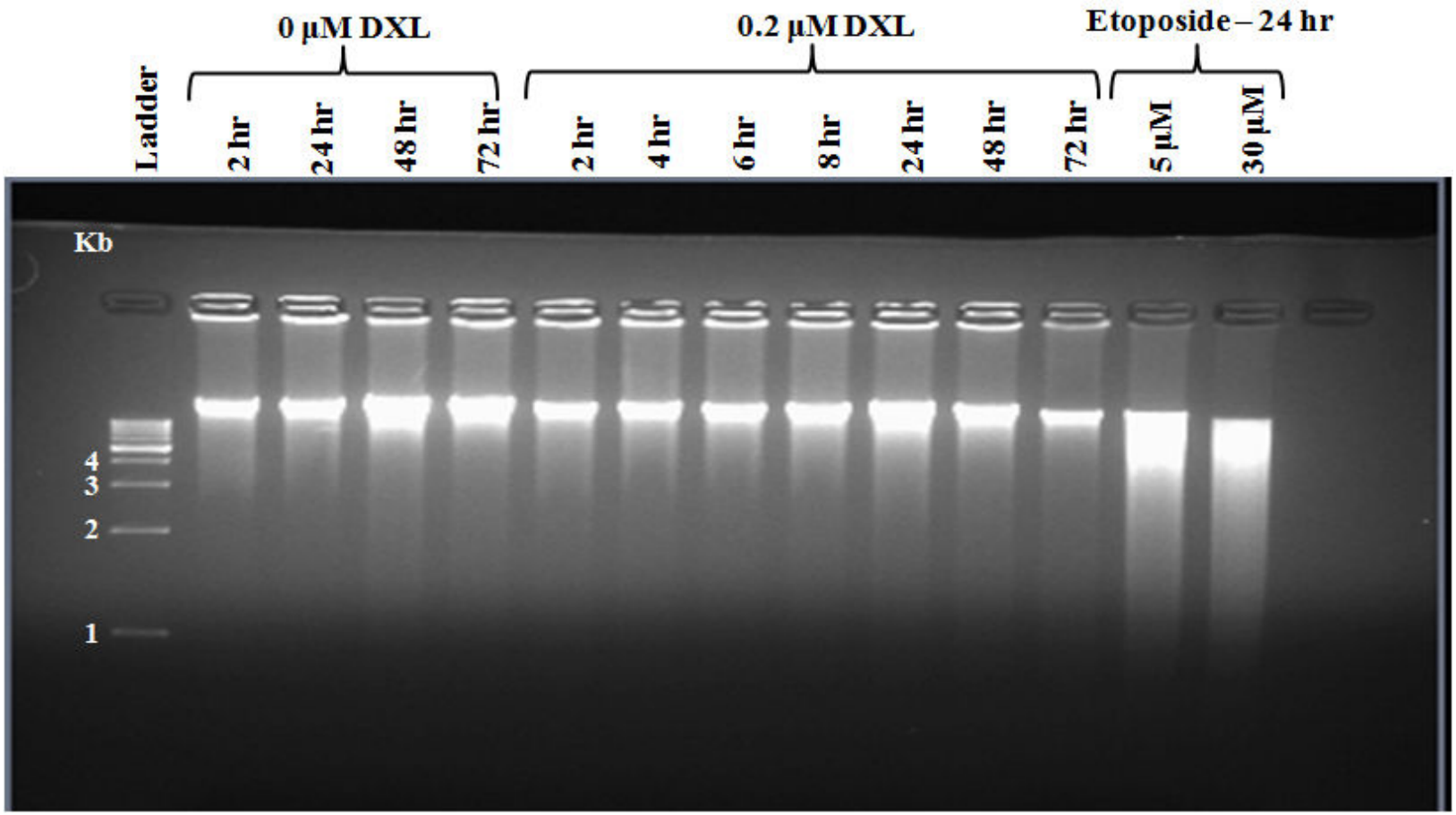

Figure 14. Agarose gel electrophoresis of DNA isolated following treatment with 0 or 0.2 µM docetaxel at several time points. The two last lanes represent positive controls for apoptosis (Jurkat cells treated with 5 µM and 30 µM of Etoposide).

3.7 Western Blot Analysis

In order to assess if apoptosis is occurring in cells treated with docetaxel and may be playing a role in rRNA disruption, immunoblotting was performed using caspase-3 and PARP-1 antibodies on lysates from untreated cells (0 μM – 24 hr) and 0.2 μM docetaxel-treated cells cultured for 24, 48 and 72 hr. Based on the western blot results shown in Figure 15A, it is evident that treatment with docetaxel results in caspase-3 and PARP-1 cleavage. Cleaved caspase-3 is observed in untreated samples, possibly due to the basal levels of apoptosis occurring in any cell population, however, by exposing the cells to drug and increasing drug exposure time, it is evident that the full length pro-caspase is decreasing, whereas the expression of cleaved caspase-3 is retained at even 72 hr of treatment. In contrast to caspase-3, PARP-1 cleavage is only observed for 0.2 μM treated samples at 24 and 48 hr. Although caspase-3 and PARP-1 cleavage displayed different patterns, the cleavage bands present at 24 and 48 hr, coincide with rRNA disruption also observed at these time points. Interestingly, at 72 hr of treatment with docetaxel, both uncleaved and cleaved PARP-1 are no longer observed, possibly due to further cleavage of these proteins. As well, the pro caspase-3 protein band is not apparent in the 72hr treated sample. An anomaly was also observed for the loading control GAPDH, which also displayed heavily reduced expression at 72 hr. Because we thought GAPDH expression might be affected as a result of treatment, we attempted to use the cytoskeletal protein β-actin as a loading control, and found that the expression of β-actin was also altered at 72 hr. The loss of PARP-1 and uncleaved caspase-3 expression at 72 hr coincides with loss of β-actin and heavily reduced GAPDH expression at 72 hr docetaxel treatment. To account for the changes in β-actin and GAPDH expression observed at 72 hr, Coomassie blue staining of an equivalent gel (Figure 15B) was performed to determine if a change in overall protein expression

was present at 72 hr. In Figure 15B, Coomassie blue staining shows that despite equal loading of protein, it is possible to observe changes in the protein profile as a result of increasing exposure to docetaxel. The protein profile of the control sample looks very different from the protein profile seen for the 0.2 μM – 72 hr sample. Although some bands occur at all time points, changes in expression are observed as a result of increasing drug exposure time.

A.

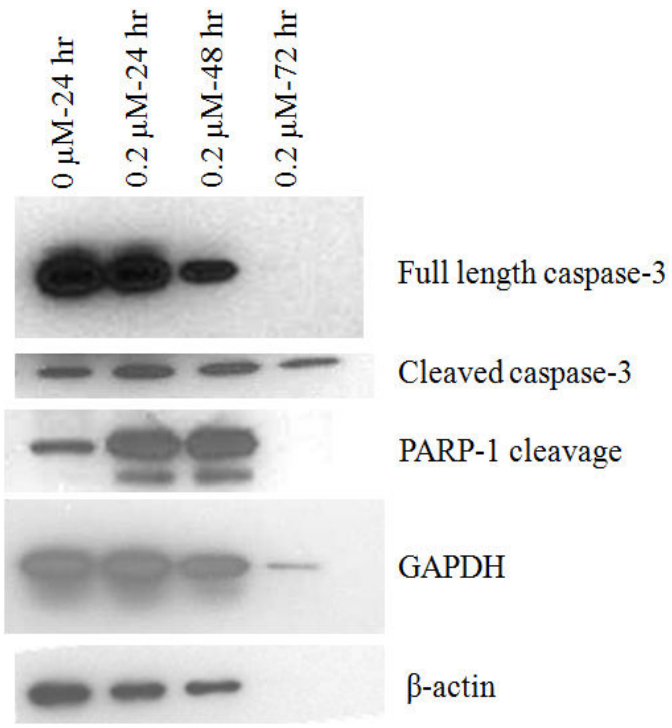

B.

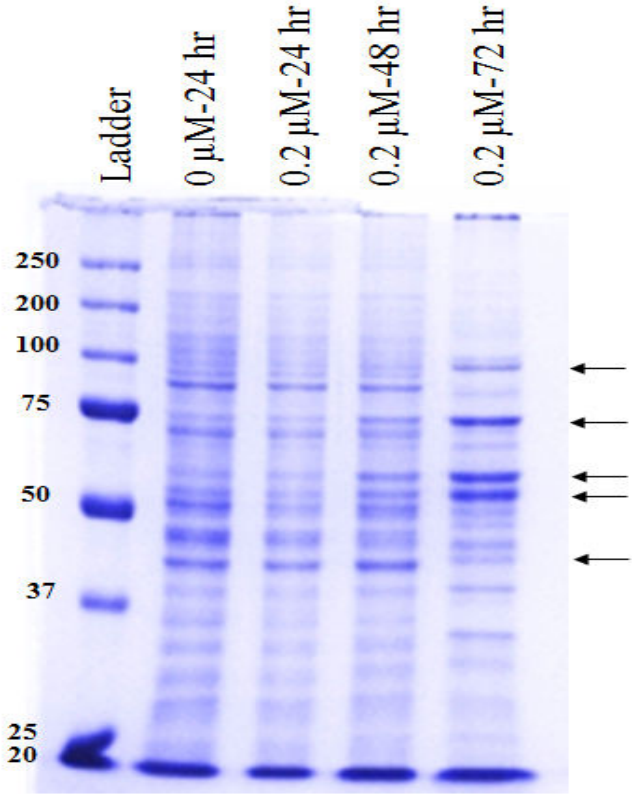

Figure 15. Immunoblotting using antibodies against full length and cleaved caspase-3 and PARP-1 for cell lysates of 0 µM – 24 hr and 0.2 µM docetaxel exposure for 24, 48 and 72 hr (A). Blots were probed with GAPDH and β-actin for loading control. Coomassie staining of the samples shows equal protein loading, however a change in protein profile is observed as a result of treatment (B). The arrows in (B) indicate representative changes in protein expression present at 72 hr.

3.8 Caspase-3 Activity Assay

The cleavage of caspase-3, which usually indicates caspase activation and which was observed in the immunoblots, was confirmed as indicating activation of capsase-3 using a caspase-3 activity assay kit (BioVision Inc, Milpitas, CA, USA). Activated caspase-3 has substrate specificity for the DEVD amino acid sequence. This substrate specificity permits the use of a chromophore-labelled DEVD peptide, to assay the activity of caspase-3 by measuring increase in absorbance by spectrophotometric detection of release of the chromophore upon cleavage from the substrate. This experiment was performed in triplicate. As rRNA disruption is evident at 24, 48 and 72 hr exposure with 0.2 μM docetaxel based on the Bioanalyzer results (Figure 10a), caspase-3 activity was measured at these time points and the results are shown in Figure 16. A significant increase in caspase-3 activity is observed for all the treated samples when compared to 0 μM samples at each time point [24 hr ($p = 0.01$), 48 hr ($p = 2.67 \times 10^{-3}$) and 72 hr ($p = 1.13 \times 10^{-2}$)]. There are no changes observed when comparing the activity measured for 0.2 μM docetaxel across the different time points. Interestingly, the 0 μM sample at 72 hr appears to have an increased activity compared to 24 or 48 hr, possibly due to apoptosis caused by nutrient exhaustion as a result of the long incubation period.

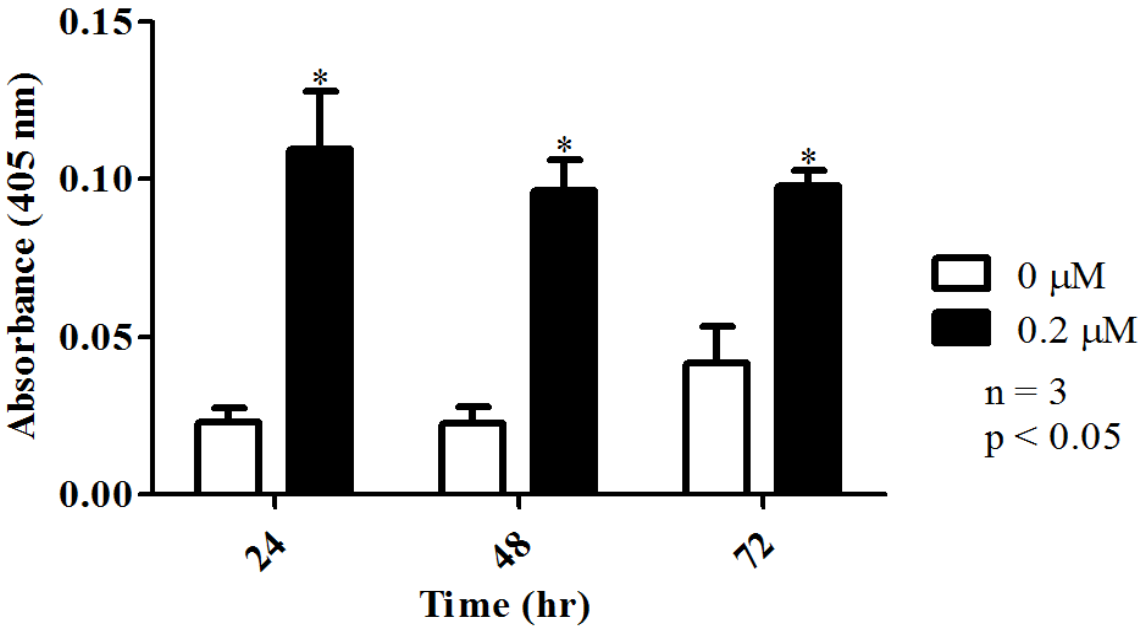

Figure 16**.** Induction of caspase-3 activity by docetaxel treatment across 24, 48 and 72 hr exposures. Asterisks denote a significant difference between treated and untreated sample at each time point.

3.9 Impact of Caspase-3 Inhibitor on rRNA Disruption

Since treatment with docetaxel results in increased caspase-3 activity and increased rRNA disruption, it becomes interesting to determine if caspase-3 activation is associated with rRNA disruption. Hence, a caspase-3 inhibitor, Q-DEVD-Oph, was used. Initially, to determine the effectiveness of the inhibitor, cells were treated with 0.2 μM of docetaxel in the presence or absence of the inhibitor. The extent of inhibition was then determined by measuring caspase-3 activity and the results are reported in Figure 17A. This experiment was performed in triplicate. We observe that the inhibitor does not significantly inhibit caspase-3 activity at 24 and 48 hr ($p = 0.41$ and $p = 0.42$), although some degree of inhibition occurs as shown in the bar graph. However, a significant decrease in caspase-3 activity is observed at 72 hr ($p = 1.06 \times 10^{-2}$). In an effort to determine if the increase in caspase-3 activity is associated with the observed RNA disruption, cells were treated with caspase-3 inhibitor at the time of treatment and the RNA was extracted and analyzed following each of the treatment time points. From the gel image shown in Figure 17B, it is evident that in the presence of the caspase-3 inhibitor RNA disruption is reduced. With the use of the inhibitor, there is a considerable reduction in the intensity of the unique disruption bands observed, and the 28S and 18S rRNA bands significantly increased in intensity. The rRNA electropherogram pattern shows distinct peaks for intact 28S and 18S rRNA, as well as for the novel peaks (labelled a, b, c and d) as shown in Figure 17C. Comparing the two electropherograms, it is obvious that the rRNA disruption resulting from treatment with docetaxel (panel a) is partially restored with the use of the caspase-3 inhibitor (panel b), where it is evident that the inhibitor augmented the size of the 28S and 18S rRNA peaks, while reducing the size of the unique disruption band peaks. Using the Agilent software, fluorescence values for each of the peaks were obtained and analyzed, and the resultant bar graph is shown in Figure 18.

The peak values demonstrate a significant increase in the fluorescence of the intact 28S ($p = 1.26 \times 10^{-3}$) and 18S ($p = 5.69 \times 10^{-3}$) peaks, as well as significant reductions in the peaks labelled b ($p = 4.46 \times 10^{-2}$) and d ($p = 1.69 \times 10^{-2}$) by using the caspase inhibitor. These results suggest that caspase-3 activation plays a role in the disruption of rRNA and that the rRNA disruption bands observed may be a product of the 28S and 18S rRNA bands.

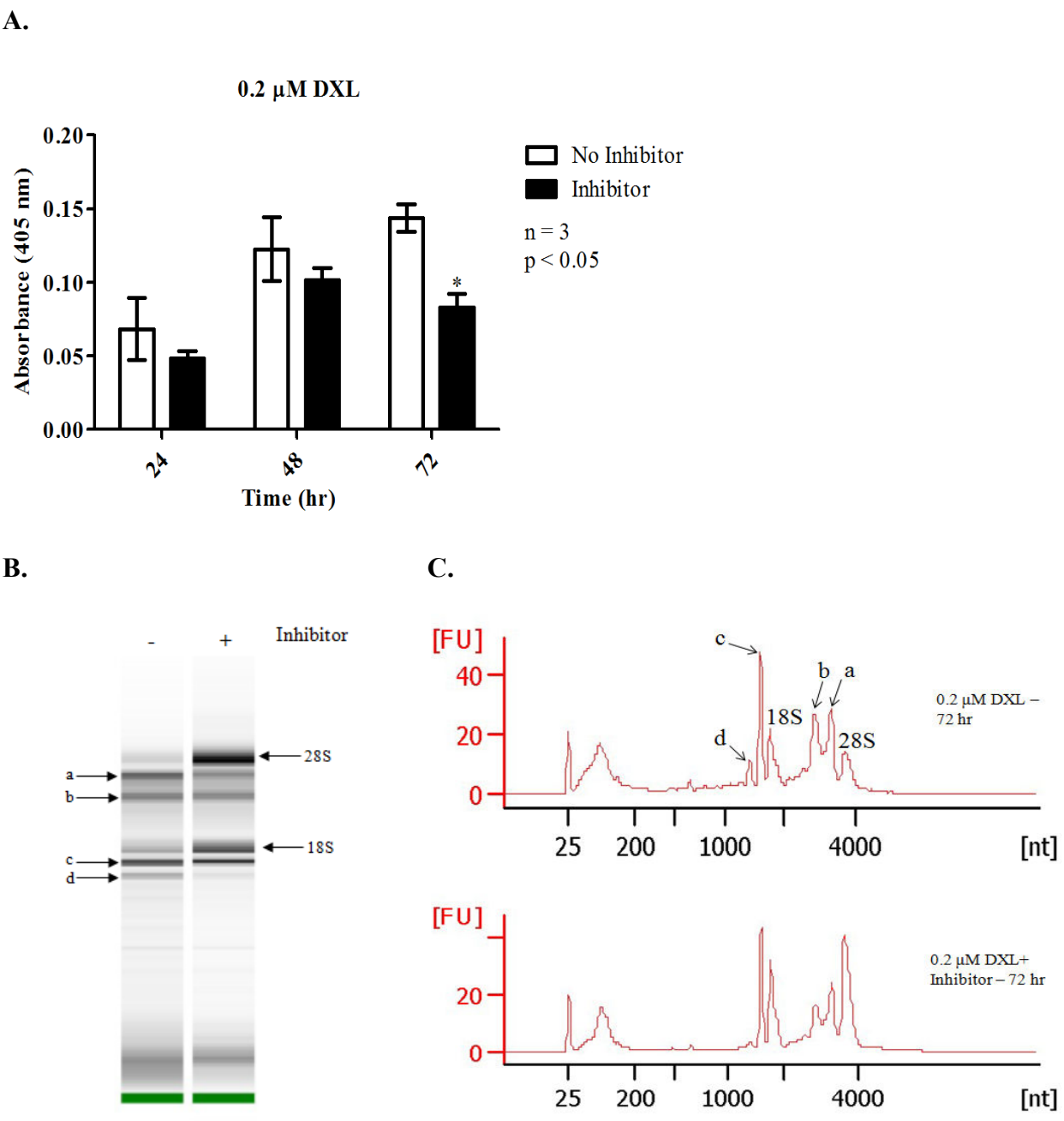

Figure 17. The effect of caspase-3 inhibitor on RNA disruption. A) Effectiveness of the inhibitor on caspase-3 activity. B) An individually scaled gel image of the RNA banding pattern of drug treated cells in the absence and presence of the inhibitor. C) Representative electropherograms of RNA isolated from A2780 cells treated with 0.2 µM DXL for 72 hours in the absence (upper panel in C) or presence (lower panel in C) of the caspase inhibitor.

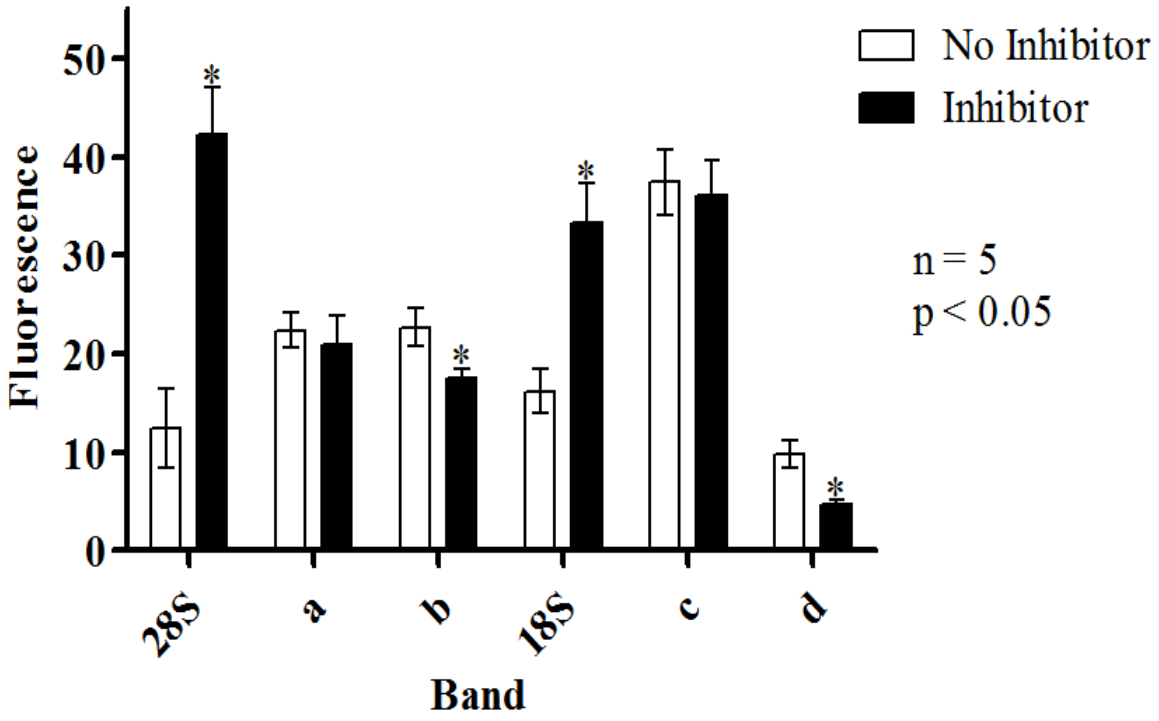

Figure 18**.** The changes in the fluorescence values of intact 28S and 18S rRNA, as well as the disruption peaks, as a result of treatment with 0.2 μM DXL for 72 hours in the absence or presence of the caspase-3 inhibitor. A significant increase in the fluorescence value for 18S and 28S rRNA peaks and significant reductions in some of the disruption bands (b and d) are evident.

3.10 Lack of Docetaxel–Induced rRNA Disruption in the A2780DXL Resistant Cells

To determine if rRNA disruption can be used as a biomarker of response to treatment with docetaxel, drug dependent rRNA disruption was investigated in docetaxel-resistant A2780 cells. Both A2780 and A2780DXL (docetaxel resistant) cells were treated with 0.005 and 0.2 μM docetaxel for 48 and 72 hr and RNA from these cells was analyzed using capillary electrophoresis. The A2780 cells treated with docetaxel show the rRNA disruption pattern previously observed, as shown in Figure 19. However, when the A2780DXL resistant cell line is treated with docetaxel, the disruption pattern is not apparent, even at the higher dose and time exposures. Absence of the unique disruption pattern observed in docetaxel resistant cell line indicates the potential use of RNA disruption as a biomarker to differentiate between chemotherapy-responsive and chemotherapy-resistant tumour cells.

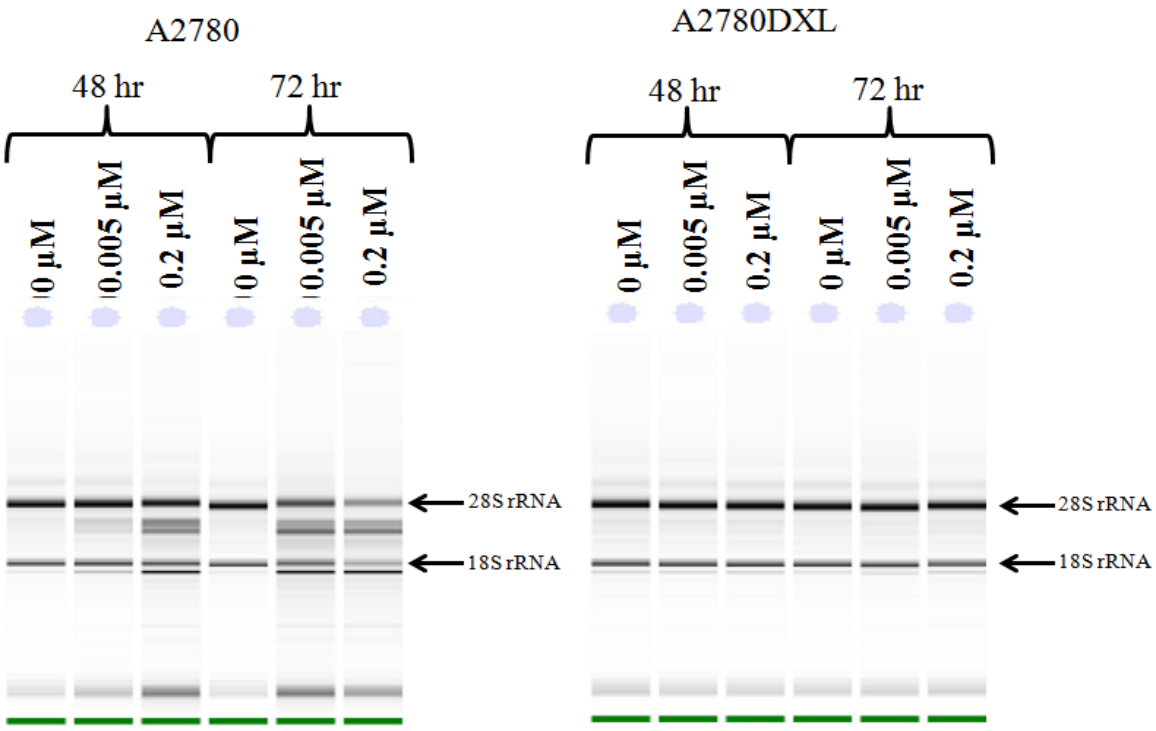

Figure 19**.** RNA quality of A2780 and A2780DXL cells treated with 0, 0.005 and 0.2 µM DXL for 48 and 72 hr. The unique bands that appear as a result of treatment in the sensitive A2780 cell line are absent in the drug- resistant A2780DXL cell line as seen in the gel images (individual scaling). The images are representative of three biological replicates.

4.0 Discussion

Due to the development of resistance and recurrence of disease observed in patients treated with chemotherapy agents, there is a need for reliable biomarkers that are able to distinguish between responding and non-responding tumours. Despite the significant progress in identifying potential mechanisms of action and resistance to taxanes, both *in vitro* and *in vivo*, currently, there are no reliable biomarkers that can predict or identify response to a taxane-based chemotherapy regime. The MA22 clinical trial is one of few trials that assessed tumours of patients pre-, mid-, and post treatment in order to identify potential biomarkers of response to chemotherapy [82]. Although earlier studies had shown that chemotherapy agents interfered with ribosome biogenesis [89], the clinical trial conducted by Parissenti et al., is the first study to show that treatment with cytotoxic chemotherapy agents such as epirubicin and docetaxel can induce RNA degradation in patients [82].

We recently surveyed a wide variety of cell lines and chemotherapy agents for their ability to induce rRNA disruption *in vitro*. One such cell line that exhibited chemotherapy-dependent rRNA disruption was the A2780 ovarian carcinoma cell line. Both taxanes (docetaxel and paclitaxel, as shown in the current study) and carboplatin (unpublished observations) showed ability to induce rRNA disruption. Considering that the current standard treatment for ovarian cancer patients includes combination chemotherapy consisting of a platinating agent and a taxane [91], we felt this was a very useful *in vitro* model system to study chemotherapy-dependent RNA disruption. We are able to demonstrate that both docetaxel and paclitaxel can strongly and reproducibly induce RNA disruption. Furthermore, because dose dependent changes in RNA disruption were observed in tumours of breast cancer patients by Parissenti et al. [82], the objective of this study was to: a) assess whether docetaxel-induced RNA disruption was dose-

and time-dependent *in vitro*, b) to determine whether RNA disruption that is present in drug-sensitive A2780 cells would be absent in the docetaxel resistant A2780DXL cell line, and c) to derive insight into the possible cellular mechanisms associated with chemotherapy-dependent RNA disruption, including its possible link to apoptosis.

4.1 Dose Dependent Changes in rRNA in Response to Docetaxel

In order to evaluate the effectiveness of docetaxel treatment and to identify if it can induce RNA degradation *in vitro*, A2780 cells were treated with increasing concentrations of docetaxel for 24hr time period before assessing cell counts, RNA quantity and integrity. Taxanes belong to a class of cytotoxic drugs that inhibit microtubule depolymerisation, which can lead to cell death. Therefore, to determine the effectiveness of docetaxel treatment, the number of intact cells (trypan blue excluding) present was counted following 24 hr of drug exposure. As seen in Figure 1, it is apparent that treating with docetaxel, at concentrations as low as 0.001 μM results in a significant drop in the number of intact cells present after 24 hr exposure. The number of intact cells is reduced further with 0.005 μM treatment, however, at higher docetaxel concentrations the intact cell count remains approximately the same. Since the sample labelled 0 – 0 hr indicates the number of cells present at the time of treatment, by comparing this sample to the samples treated with 0.005 – 40 μM docetaxel for 24 hr, it can be seen that some cells have died, although, no dose dependent decrease in intact cell count is observed for these concentrations. Although trypan blue has the ability to detect cells with intact membranes, it cannot distinguish between viable and non viable cells, because cells may have damaged metabolic pathways or small surface alterations that may not be detected by trypan blue staining [92]. Therefore, although we do not see a dose dependent decrease in intact cell count, this does not necessarily mean that the cells continue to be viable. Comparing the intact cell count at

0.001 μM DXL to the cell numbers at 0 – 0 hr it is possible to observe a small increase in the number of intact cells, indicating that the lower docetaxel concentration of 0.001 μM is possibly not enough to completely cause cell cycle arrest within a 24 hr period. However at the higher concentrations, the drug is able to cause a block in cell cycle progression, yet not enough to induce cell death in the 24 hr drug exposure period. Similar observations were reported by Wang et al. in 2008, where treatment with paclitaxel for 24 hrs resulted in an inhibitory effect of cell growth at higher drug concentration, which gradually lead to a change in cell morphology and death [93].

We also assessed changes in RNA quantity and quality as a result of treatment with increasing concentrations of docetaxel for a 24 hr period. A biphasic trend is observed for RNA concentration, as we see a drop in RNA concentration until 0.2 μM docetaxel treatment (Figure 2A). When comparing the graph for RNA concentration in Figure 2A to the cell counts in Figure 1, we notice that the cell counts drop significantly at 0.001 μM docetaxel concentration and although they decrease further, they remain approximately the same for higher drug concentrations. However, similar changes were not observed for RNA concentration. To try to understand how these observations might be related, the RNA content per cell was determined by dividing the amount of RNA by the total number of cells present (intact, as well as those that stained with trypan blue) following docetaxel treatment. As seen in Figure 3, compared to both the 0 μM samples, all the docetaxel treated samples have increased RNA per cell. It is a well known phenomenon that in preparation for cell division, cells increase in size and synthesize RNA, DNA and proteins [94]. However, since treatment with taxanes blocks depolymerisation of microtubules and results in mitotic arrest, large cells are formed with about twice the typical cellular RNA content, that are unable to divide into two daughter cells. Several studies have

reported the observation of large multinucleated cells as a result of treatment with taxanes [95], and the increased amount of RNA per cell, noted as a result of docetaxel treatment in this study, may be a reflection of that phenomenon.

The CAN-NCIC-MA22 clinical trial by Parissenti et al., was the first study to show that cytotoxic chemotherapy agents not only induce RNA degradation in patients, but also that there is an association between tumour RNA integrity (RIN) and positive patient response to treatment. The study also reported that low RIN values mid-treatment were correlated with high drug doses, which later lead to pathological complete response in patients post-treatment. The RIN value is a numerical representation of the quality of RNA sample on a scale of 1 to 10, where10 represents intact RNA and 1 represents completely degraded RNA [96]. A change in RIN as a result of treatment with increasing concentrations of docetaxel was assessed in the current study (Figure 2B). Although there is a trend for the RIN values to decrease up to the 0.2 μM docetaxel concentration, the values appear to increase at docetaxel concentrations higher than 0.2 μM. Significant difference in RIN was only observed for high drug concentrations of 30 and 40 μM where a drop in RIN is observed, although the RIN values still remain high (close to RIN of 10). To determine the extent of RNA disruption, we also looked at the electropherogram traces (Figure 4a) as well as the gel image (Figure 5a) generated following capillary electrophoresis on an Agilent Bioanalyzer. Interestingly, discrete bands (and peaks) consistently appeared in the rRNA banding pattern as a result of drug treatment at various concentrations of docetaxel just below the 28S and 18S rRNA bands. The unique bands become visible at 0.005 μM docetaxel and persist up to 30 μM docetaxel, appearing to be the strongest with 0.2 μM docetaxel treatment. The increase in RIN observed at the high drug concentrations is likely due to the loss of these unique disruption bands, allowing the remaining material in the 28S and 18S

rRNA peaks to be used in the calculation of the RIN value, as seen in the gel image and peak traces.

4.2 Time Dependent Changes in rRNA in Response to Docetaxel

Based on the results of the dose experiments, it became apparent that the strongest novel disruption RNA bands occurred between 0.005 and 0.2 μM docetaxel. Therefore, these two concentrations were selected to study changes in RNA integrity over time. Similar to the dose experiments, the effect of length of exposure on docetaxel-induced RNA disruption was assessed by determining cell counts, RNA quantity and RNA integrity. At the earlier time point of 8 hr, no significant difference was observed for the various treatment conditions in terms of intact cell count, RNA quantity, RNA per cell or RIN. Because taxanes inhibit cell proliferation by binding to microtubules and suppressing microtubule dynamics, cells would be most sensitive to taxane treatment when undergoing mitosis [97]. Since the A2780 cell line has been reported to have a doubling time of 19.8 hr [43], and due to the fact that cells were not synchronized prior to treatment and did not have a chance to undergo at least one cell division, no significant cytotoxic effects of docetaxel were observed following 8 hr of treatment. At the later time points of 24, 48 and 72 hr, we observe significantly fewer numbers of intact cells as a result of treatment, with the most significant difference observed at 72 hr and with the higher drug dose used (Figure 6).

In terms of RNA concentration (Figure 7A), a significant decrease is observed at 48 and 72 hr for 0.2 μM docetaxel. However, for 0.005 μM treatment, a significant drop in RNA concentration is observed only at 72 hr of exposure. This decrease in RNA concentration may be associated with the decrease in cell counts that are observed at the longer exposure time. In contrast to the RNA concentration, we observe an increase in the amount of RNA per cell for 0.2 μM docetaxel at 24, 48 and 72 hr exposure. Similar to the change in total RNA concentration, a

significant increase in RNA per cell for 0.005 μM sample is observed only for the 72 hr exposure. Significant decreases in RIN are observed with 0.2 μM treatment starting at 24hr, however, for 0.005 μM docetaxel treatment, RIN values do not drop significantly until 48 and 72 hr. These results show time dependence of RNA disruption in terms of RIN values due to docetaxel treatment, which are also seen in the electropherogram traces and in the gel images in Figure 9a and Figure 10a. The RNA banding patterns for the different exposure times show that the disruption bands do not appear until at least a 24 hr exposure, and that they are stronger for the higher drug dose at each time point. At 72 hr exposure, the 28S and 18S bands become faint, where as the unique bands appear to increase in intensity. Although not using chemotherapy agents, other researchers have observed rRNA degradation bands as a result of using apoptosis inducing agents such as glucocorticoids, okadaic acid, TNF, cycloheximide, deoxynivalenol and the calcium ionophore A23187, where the degradation bands were found to originate from the 28S rRNA, as revealed using labelled oligonucleotide probes [87, 98, 99]. It is possible that the disruption bands appearing coincident with taxane treatment are a result of degradation of the 28S and 18S bands; however, this claim can not be conclusively made on the basis of gel image alone. The generation of 28S rRNA degradation products by apoptosis-inducing agents in the above mentioned studies argues against the hypothesis that the abnormal rRNA bands are simply the result of changes in secondary or tertiary structures of the rRNAs.

4.3 rRNA Disruption in Response to Paclitaxel Treatment

Paclitaxel and docetaxel both share a similar mechanism of action; however, variations in terms of toxicity and efficacy have been observed before [100]. Docetaxel has also been reported to have a higher affinity for microtubules compared to paclitaxel [24]. Because the two taxane drugs appear to share many features, a comparison of the effect of paclitaxel on RNA integrity

was performed. As a result of paclitaxel treatment, similar rRNA disruption banding pattern was observed and found to be dose (Figure 4b and Figure 5b) and time dependent (Figure 9b and Figure 10b) in the A2780 cell line. We see that similar to the dose dependent RNA disruption observed for docetaxel, the aberrant disruption bands were most apparent for certain paclitaxel concentrations. Further disruption of the unique bands possibly explains the lack of unique bands observed at high drug concentrations of 10 – 40 μM paclitaxel, and we also notice that the intensity of the 18S and 28S rRNA peaks or bands decrease at the high drug concentrations. The time dependence of paclitaxel induced RNA disruption was also assessed, and found to be similar to docetaxel, where treatment at later time points resulted in the most disruption. Interestingly, two aberrant bands are observed below the 18S rRNA band as a result of paclitaxel treatment, where as docetaxel treatment resulted in only one band below the 18S rRNA, indicating that the two drugs have slightly different effects on rRNA disruption.

4.4 Cell Cycle Arrest and Early Apoptosis Induction is Associated with rRNA Disruption

Taxanes are considered mitotic poisons because they bind to β-tubulin monomers, resulting in the stabilization of microtubules and inhibiting their depolymerisation [101]. As a result, cell cycle progression is blocked; however, it is unclear if there is an association between mitotic arrest and the induction of cell death by apoptosis. The mechanism of cell death, activated as a result of treatment with docetaxel, has been shown to be dependent on drug concentration [102]. In this study, we observed that 0.2 μM of docetaxel is able to induce mitotic arrest starting at 8 hr of exposure (Figure 11B). Similar observations were made by Hernandez-Vargas et al., where treatment of breast carcinoma cell lines with 0.1 μM of docetaxel resulted in cell cycle arrest starting at 8 hr [102]. Based on our experimental conditions, we see cells accumulating in the G_2/M phase as early as 8 hr, whereas by 24 hr almost all of the cells are

found to be arrested in this phase. Additionally, we begin to observe an increase in the sub G1 peak after 24 hr of docetaxel exposure; whereas Hernandez-Vargas et al. reported only a small increase in the sub G1 peak using similar docetaxel concentrations in breast cancer cell lines [102]. When cells are undergoing apoptosis, the cell, including the nucleus, can undergo fragmentation into discrete bodies, called apoptotic bodies [103]. These bodies, observed as distinct sub G1 peaks in plots of fluorescence intensity versus cell number generated by the flow cytometer, contain hypodiploid DNA content. In the current study, the hypodiploid cells become more prominent at 48hr, but following 72 hr exposure, almost all "cells" had sub G1 DNA content (Figure 11B). Although our experiments show an increase in cells containing a hypodiploid DNA content, previous reports have suggested that the appearance of a sub G1 peak may be a result of nuclear aberrations or debris [104], and therefore needs to be further validated using other techniques to determine the role of apoptosis. In the current study, the induction apoptosis was further validated using annexin-V and propidium iodide (PI) staining. It is well established that apoptosis is accompanied by changes in the plasma membrane structure, resulting in the exposure of phosphatidylserine to the outer leaflet of the cell membrane [105]. Surface exposure of phosphatidylserine is then detected using annexin-V, a phospholipid binding protein that has a high affinity for phosphatidylserine [106]. Our results indicate that the appearance of a sub G1 peak after 24 hr of docetaxel exposure is accompanied by an increase in the number of annexin-V-positive, PI-negative cells, indicative of early apoptosis (Figure 12). Similar to the time dependent increase in the sub G1 peak, we also observe an increase in early apoptotic cells as a result of increased drug exposure time. This is concurrent with the appearance of the rRNA disruption bands after docetaxel treatment (Figure 9a and Figure 10a). In summary, we observed a significant increase in the number of early apoptotic cells, and the

sub G1 peak at the 48 and 72 hr exposure times, similar to the increase in rRNA disruption observed by increasing the length of docetaxel exposure.

4.5 Recovery and Proliferation of Cells Undergoing Treatment

Although exposure of phosphatidylserine on the surface of cells undergoing apoptosis is typically associated with the initiation of the apoptotic process, it has been observed in the absence of apoptosis [107] and has also been reported to be a reversible phenomenon, not associated with other apoptosis markers such as DNA fragmentation in certain cell lines [108]. Similarly, the presence of a sub G1 peak is not a proof of apoptotic cell death alone, as a hypodiploid cellular DNA content might indicate groups of chromosomes or nuclear debris [104]. Therefore, we decided to determine the proliferative ability of cells in drug-free medium following treatment of cells with docetaxel for various lengths of time in order to assess if the cells are able to recover, or are on a path of cell death. Although annexin-V staining and cell cycle analysis was only performed for 0.2 μM docetaxel treatment, a lower concentration of docetaxel (0.005 μM) was used in addition to a no drug control to determine differences in cell proliferation as a result of drug treatment. We found that cells treated with the lowest drug concentration are able to recover after 24 and 48 hr of drug treatment, however at a much slower rate after 48 hr in 0.005 μM of drug (Figure 13). At 72 hr of treatment, cells are unable to recover, even after a 96 hr recovery period. When the higher drug concentration of 0.2 μM docetaxel is used, cells are unable to recover even after only 24 hr of drug exposure (Figure 13). Similar changes were reported by Li et al., where treatment with docetaxel showed a dose- and time-dependent inhibition in cell proliferation in two prostate cancer cell lines [109]. Although rRNA is extremely stable, under physiological conditions such as starvation, ribosome degradation can occur, leading to slow cell growth [110]. Since rRNA disruption is observed for

these two drug concentrations (Figure 10a), it might be concluded that the loss of cell proliferation observed as a result of treatment might be occurring due to the rRNA degradation, since the unique disruption bands start to appear at 24 hr with 0.2 μM docetaxel treatment. Along with the lack of cell proliferation, we observe a significant increase in early apoptotic cells (annexin-V+, PI-) and a sub G1 peak starting at 24 hr as a result of treatment with 0.2 μM docetaxel. Also interesting to note is that, when cells were counted as a result of treatment with 0.2 μM DXL at 24 hr (Figure 1), a significant number of intact cells were observed following treatment, but these cells were unable to proliferate as seen in the recovery assay (Figure 13a), indicating that not all trypan blue excluding cells are viable. Previous reports have indicated that degradation of 28S and 18S rRNA was observed as a result of treatment with cytotoxic agents, and that it was accompanied by DNA fragmentation, demonstrating that rRNA degradation occurs in conjunction with apoptosis [86].

The degradation of DNA into internucleosomal fragments is another well-known hallmark of apoptosis. Although several studies have reported that docetaxel treatment results in DNA fragmentation, which subsequently leads to cell death [111, 112], we were unable to detect any DNA degradation (Figure 14) even at the later treatment times where an increase in early apoptotic cells (annexin-V+/PI-) was observed (Figure 12). Although a well-accepted phenomenon, apoptosis has been reported to occur in the absence of DNA fragmentation [113, 114]. In a renal carcinoma cell line, although apoptosis induction was reported to be accompanied by the activation of caspases and PARP cleavage, a lack of oligonucleosomal fragments was noted [114], indicating that cells can undergo apoptotic cell death without the well-established, characteristic feature of apoptosis, DNA fragmentation.

4.6 Role of Caspase-3 and PARP-1 in rRNA Disruption

In the current study, because the unique rRNA disruption bands coincide with suppression or loss of cell proliferation and seem to be accompanied by some apoptotic markers such annexin-V staining, we assessed the role of activation of certain apoptotic proteins and determined their association with the chemotherapy dependent rRNA disruption we observed. Since RNA degradation of only the 28S rRNA [84, 85] and of both the 18S and 28S rRNA [86] has been previously observed to occur when cells are undergoing apoptosis, the role of apoptosis in docetaxel dependent rRNA degradation was evaluated by assessing cleavage of caspase-3 and PARP-1. Rather than determining whether docetaxel treatment is activating the intrinsic or extrinsic apoptotic pathway, cleavage of caspase-3 was studied as it is activated by both apoptotic pathways [115]. In a study by Mhaidat et al. published in 2007, treatment of melanoma cells with docetaxel resulted in caspase-3 cleavage after 24 hours of treatment [116]. Based on our current experimental conditions, caspase-3 cleavage is observed as early as 24 hr following treatment with 0.2 μM docetaxel, similar to when the rRNA disruption is observed (Figure 15A). Following 72 hr of treatment, no uncleaved caspase-3 is observed, and only the cleaved product is apparent. Although it is unexpected to observe a complete loss of the procaspase while the cleaved product persists, it is possible that disruption of rRNA observed is associated with loss of translation capacity, which might also explain the changes in total protein profile seen using Coomassie staining (Figure 15B). Due to the changes in protein profile observed as a result of increased docetaxel exposure time, we wished to confirm the persistence of caspase-3 activation using a caspase-3 activity assay kit. Compared to the no drug control, a significant increase in caspase-3 activity was observed at 24, 48 and 72 hr of 0.2 μM docetaxel treatment confirming the western blot results (Figure 16). Similar results were reported by Mediavilla-Varela et al.,

where treatment of prostate cancer cells with 0.1 μM docetaxel showed a trend of time dependent increase in caspase activity at 24 and 48 hrs [27]. In cells undergoing apoptosis, activation of caspase-3 leads to the cleavage of other proteins resulting in the biochemical and morphological markers of apoptosis [117]. PARP-1 which is normally involved in DNA damage repair, is cleaved by caspase-3 during degradation of cellular DNA in cells undergoing apoptosis, thus preventing DNA damage repair. Using our current experimental conditions, we observe PARP-1 cleavage at 24 and 48 hr of treatment; however no PARP-1, cleaved or uncleaved, is observed at 72 hr (Figure 15A). Similarly, PARP-1 cleavage as a result of docetaxel treatment has been observed by others [118]; however, the effect of prolonged exposure to docetaxel resulting in the loss of PARP-1 detection is not often documented. As mentioned previously, the observations made in this study may be related to the rRNA disruption observed, as ribosome degradation may possibly result in loss of translational capacity in the cell, resulting in no PARP-1 detection at the later treatment time point. Since the cleavage of caspase-3 and PARP-1 are concurrent with the appearance of the unique rRNA disruption bands, it is possible that these two phenomena may be related.

The results from Coomassie staining (Figure 15B) show a time dependent change in protein expression state, indicating that at the later time point, chemotherapy is causing a change in cellular metabolism. We observe that some bands that are present at the earlier time points are absent as a result of treatment with 0.2 μM docetaxel at 72 hr, indicating loss of protein either due to degradation or lack of synthesis. In the literature, there is no evidence of docetaxel treatment resulting in changes in GAPDH or β-actin levels. Treatment of human epithelial ovarian carcinoma cells SKOV3 and HeyA8 [119], and human prostate cancer cells LNCaP [109] with docetaxel for 48 and 72 hr did not show any changes in β-actin levels. It is possible

that protein profile changes that are observed in the current study may be a result of the relatively high drug concentration being used, and is cell line specific. Also, since treatment with docetaxel results in a time dependent increase in rRNA disruption (Figure 9a and Figure 10a), it is likely that the temporal changes in total protein profile observed in the current study (Figure 15B) may likely be due to a loss of ribosome function, which could lead to a reduction in protein production and change the total protein profile in a cell.

To determine whether the initiation of apoptosis and rRNA disruption are related events, cells were treated with a caspase-3 inhibitor at the time of treatment. The inhibitor used Q-DEVD-Oph (BioVision Inc, Milpitas, CA, USA), works by irreversibly binding to active caspase-3 and blocking any downstream events [120]. We found that the inhibitor was significantly inhibiting caspase-3 activity, but only at 72 hr of drug treatment (Figure 17A). Similarly, a significant change in the rRNA banding pattern was observed only at the 72 hr treatment time point, which showed that using the inhibitor reduced the appearance of some of the aberrant rRNA bands, and that the intensity of the intact 18S and 28S rRNA bands increased significantly (Figure 17B and Figure 18). In a study published in 2000 by King et al., a small reduction in 28S rRNA degradation was observed a result of using just a caspase-3 inhibitor, however using the pan caspase inhibitor, ZVAD, resulted in the most protective effect, preventing any degradation of the ribosomal RNA [87]. A recent study published in 2012 also reported that using a pan caspase inhibitor resulted in significant reduction of rRNA degradation bands that appear due to treatment with ribotoxins [121]. Based on the results obtained using a caspase-3 specific inhibitor, which show that complete inhibition of rRNA disruption was not observed, we can only conclude that, while caspase-3 plays an important role in the chemotherapy-dependent rRNA disruption we observed, it is not wholly dependent on caspase-3

activation. However, to generalize this statement for the other caspases involved, the activity of all caspases as well as their inhibitors need to be examined to determine if the rRNA disruption observed is occurring through a caspase dependent pathway or pathways. Although caspases are often associated with apoptosis, activation of caspases may also affect non-apoptotic pathways such as cell proliferation, survival and differentiation [122]. Therefore, rRNA disruption cannot be contributed to activation of caspases alone, and other cell death pathways (e.g. autophagy, necrosis) may also need to be investigated along with the activation of other caspases to associate rRNA disruption with caspase-3 activation.

The unique bands that are result from docetaxel treatment appear similar to the 28S rRNA degradation bands reported to be induced by apoptotic agents such as glucocorticoids, okadaic acid, TNF, cycloheximide, the calcium ionophore A23187 and ribotoxins [87, 98, 99]. The bands that appear as a result of treatment in these studies were hybridized to probes derived from 18S and 28S rRNA molecules to determine the origin of the rRNA degradation bands. Although it cannot be stated conclusively, considering that the caspase-3 inhibitor restored the 18S and 28S rRNA bands in the current study, it is possible that the novel bands that result from docetaxel treatment are derived from either the 18S and 28S rRNA bands; however, this needs to be proved conclusively, for example, by using labelled probes.

4.7 Absence of rRNA Disruption in a Drug Resistant Cell Line

Since docetaxel treatment resulted in the development of aberrant rRNA bands/peaks in the A2780 ovarian cancer cell line, a drug sensitive cell line, we were interested to see whether the same results would be observed in a docetaxel resistant cell line. The A2780DXL cell line is a docetaxel resistant cell line developed and characterized by Armstrong et al., in 2012 [43]. The dose and time dependent increase in rRNA disruption observed as a result of treatment in the

sensitive cell line, was absent in the drug resistant cell line even after 72 hr docetaxel exposure (Figure 19). This indicates that the induction of rRNA disruption is an effective marker of response to chemotherapy, since no rRNA disruption was observed in the resistant cell line following chemotherapy drug exposure. Similar results were observed in the clinical trial by Parissenti et al., where significant reductions in tumour RIN values were observed in patients that responded to epirubicin/docetaxel chemotherapy [82]. It was also reported that patients who experienced a pathological complete response (pCR) in this clinical trial had low RIN values mid treatment. Based on the results from the current study and of the observations made by Parissenti et al., RNA degradation has the potential to be an efficient marker of positive response to chemotherapy.

5.0 Conclusion

Although several earlier studies have reported observations of rRNA degradation as a result of treatment with apoptosis inducing agents or ribotoxins, degradation of rRNA into unique bands has not been reported as a result of using chemotherapy drugs. We have established a highly efficient and useful *in vitro* model system to demonstrate RNA disruption by taxanes. We were able to demonstrate both dose- and time- dependent rRNA disruption in response to treatment with paclitaxel and docetaxel. In an effort to identify if the rRNA disruption is associated with apoptosis as reported by others in the literature, we were able to demonstrate that rRNA disruption observed as a result of docetaxel treatment is temporally correlated with activation of apoptosis as measured using annexin-V staining, cellular DNA content analysis, and cleavage of caspase-3 and PARP-1 proteins. Interestingly, a significant increase in the intact 18S and 28S rRNA and a decrease in the aberrant bands was observed when experiments were conducted in the presence of both a caspase-3 inhibitor and docetaxel (compared to docetaxel alone). Considering that the inhibitor restored the intensity of 28S and 18S ribosomal RNA, while concurrently decreasing the intensity of some of the disruption bands (b and d), this could indicate that the novel bands are degradation products of 28S and 18S rRNA.

By assessing if other caspases are also activated when rRNA disruption is observed, we may be able to conclude whether the changes in the rRNA banding pattern observed is occurring through a caspase-dependent apoptotic pathway. Since the appearance of the unique rRNA bands/peaks was associated with loss or suppression of cell proliferation, and since caspase-3 has been associated with non-apoptotic functions such as proliferation, differentiation, and survival [123], it is also possible that the rRNA disruption might be occurring independent of an apoptotic cell death pathway.

Although DNA fragmentation, a well accepted characteristic of both apoptotic cell death pathways was not observed, it is unclear whether the rRNA disruption is a result of activation of an apoptotic pathway. Apoptosis, although a well characterized mechanism, is cell type specific and therefore several different markers need to be assessed to accurately identify and differentiate apoptosis from other cell death mechanisms [124]. Also, different cell death pathways share certain characteristics, making it difficult to isolate and identify the exact cell death pathway activated. Since activation of caspases and other apoptotic markers without DNA fragmentation has been previously observed [114], it is possible that the rRNA disruption observed in this study as a result of taxane treatment, is associated with caspase-dependent apoptosis.

Future experiments investigating other apoptotic markers such as membrane blebbing, activation of other apoptotic genes and proteins will allow us to identify the role of apoptosis in chemotherapy dependent RNA disruption. Since several studies have reported RNA degradation occurring as a result of apoptosis induction, but DNA fragmentation is not always observed, it is possible that RNA degradation/disruption might be a more reliable indicator of apoptotic cell death or of cell death in general. Furthermore, although trypan blue excluding cells were detected in samples treated with 0.2 μM DXL for 24 hr, which could be interpreted as being viable cells, our recovery assay showed that these cells were not viable. The lack of viability in these intact cells corresponded with the presence of rRNA disruption bands in the sample, implying that RNA disruption may be a more accurate measure of viability. Other evidence that rRNA disruption is a good indicator of cell death pathways is that although we observed a loss of caspase-3 and PARP-1 cleavage at 72 hr, rRNA disruption bands are still evident at later time points. However, to better understand the mechanism of RNA disruption, other pathways also

need to be examined such as ribophagy, non fuctional RNA decay (NRD pathway) and the role of RNases as they have also been implicated in RNA degradation [83].

Furthermore, future directions should involve determining the origin of the unique rRNA bands observed in this study. Based on previous studies which reported that the RNA degradation bands were derived from 18S and 28S rRNA bands, and due to a significant recovery of 18S and 28S rRNA bands as a result of using a caspase-3 inhibitor in the current study, it is likely that the unique bands resulting from the use of taxane chemotherapy are derived from the intact rRNA bands. However, this needs to be confirmed using northern blotting technique with labelled probes of 18S and 28S rRNA.

Although we have successfully established an *in vitro* model to study taxane dependent RNA disruption, future experiments should involve determining if taxanes are able to induce RNA disruption in other cancer cell types, and also to determine if other classes of chemotherapy agents can also cause changes in rRNA banding pattern. The absence of the unique rRNA pattern observed in docetaxel resistant cell line indicates the potential use of RNA disruption as a biomarker to differentiate between chemotherapy-responsive and chemotherapy-resistant tumour cells. Since the CAN-NCIC-MA22 clinical trial reported that cytotoxic chemotherapy agents can induce RNA degradation in patients, and that the RNA degradation observed correlated with pathological complete response [82], degradation/disruption of RNA is proposed as a promising biomarker for positive response to chemotherapy agents.

References

1. Huizing, M.T., et al., *Taxanes: a new class of antitumor agents.* Cancer Invest, 1995. **13**(4): p. 381-404.
2. de Bree, E., et al., *Treatment of ovarian cancer using intraperitoneal chemotherapy with taxanes: from laboratory bench to bedside.* Cancer Treat Rev, 2006. **32**(6): p. 471-82.
3. Jennewein, S., et al., *Taxol biosynthesis: taxane 13 alpha-hydroxylase is a cytochrome P450-dependent monooxygenase.* Proc Natl Acad Sci U S A, 2001. **98**(24): p. 13595-600.
4. Vogel, C.L. and J.M. Nabholtz, *Monotherapy of metastatic breast cancer: a review of newer agents.* Oncologist, 1999. **4**(1): p. 17-33.
5. Fauzee, N.J., *Taxanes: promising anti-cancer drugs.* Asian Pac J Cancer Prev, 2011. **12**(4): p. 837-51.
6. Zhang, J.A., et al., *Development and characterization of a novel Cremophor EL free liposome-based paclitaxel (LEP-ETU) formulation.* Eur J Pharm Biopharm, 2005. **59**(1): p. 177-87.
7. Charpidou, A.G., et al., *Therapy-induced toxicity of the lungs: an overview.* Anticancer Res, 2009. **29**(2): p. 631-9.
8. Vasey, P.A., et al., *Phase III randomized trial of docetaxel-carboplatin versus paclitaxel-carboplatin as first-line chemotherapy for ovarian carcinoma.* J Natl Cancer Inst, 2004. **96**(22): p. 1682-91.
9. Maenpaa, J.U., *Docetaxel: promising and novel combinations in ovarian cancer.* Br J Cancer, 2003. **89 Suppl 3**: p. S29-34.
10. Ferlay, J., et al., *Estimates of worldwide burden of cancer in 2008: GLOBOCAN 2008.* Int J Cancer, 2010. **127**(12): p. 2893-917.

11. Jemal, A., et al., *Global cancer statistics.* CA Cancer J Clin, 2011. **61**(2): p. 69-90.

12. Aksoy, S., O. Dizdar, and K. Altundag, *Weekly paclitaxel in the adjuvant treatment of breast cancer.* N Engl J Med, 2008. **359**(3): p. 310; author reply 310-1.

13. Papademetriou, K., A. Ardavanis, and P. Kountourakis, *Neoadjuvant therapy for locally advanced breast cancer: Focus on chemotherapy and biological targeted treatments' armamentarium.* J Thorac Dis, 2010. **2**(3): p. 160-70.

14. Chan, A., et al., *New insights into the pathogenesis of ovarian carcinoma: time to rethink ovarian cancer screening.* Obstet Gynecol, 2012. **120**(4): p. 935-40.

15. Jemal, A., et al., *Cancer statistics, 2010.* CA Cancer J Clin, 2010. **60**(5): p. 277-300.

16. Yap, T.A., C.P. Carden, and S.B. Kaye, *Beyond chemotherapy: targeted therapies in ovarian cancer.* Nat Rev Cancer, 2009. **9**(3): p. 167-81.

17. Vergote, I., et al., *Neoadjuvant chemotherapy or primary surgery in stage IIIC or IV ovarian cancer.* N Engl J Med, 2010. **363**(10): p. 943-53.

18. Markman, M., *Antineoplastic agents in the management of ovarian cancer: current status and emerging therapeutic strategies.* Trends Pharmacol Sci, 2008. **29**(10): p. 515-9.

19. Watari, H., et al., *Weekly paclitaxel/5-fluorouracil followed by platinum retreatment for patients with recurrent ovarian cancer: a single institution experience.* Eur J Gynaecol Oncol, 2008. **29**(6): p. 573-7.

20. McCourt, C., et al., *Is there a taxane-free interval that predicts response to taxanes as a later-line treatment of recurrent ovarian or primary peritoneal cancer?* Int J Gynecol Cancer, 2009. **19**(3): p. 343-7.

21. Perez, E.A., *Microtubule inhibitors: Differentiating tubulin-inhibiting agents based on mechanisms of action, clinical activity, and resistance.* Mol Cancer Ther, 2009. **8**(8): p. 2086-95.

22. McGrogan, B.T., et al., *Taxanes, microtubules and chemoresistant breast cancer.* Biochim Biophys Acta, 2008. **1785**(2): p. 96-132.

23. Rowinsky, E.K., *The development and clinical utility of the taxane class of antimicrotubule chemotherapy agents.* Annu Rev Med, 1997. **48**: p. 353-74.

24. IZBICKA, E., et al., *Biomarkers for sensitivity to docetaxel and paclitaxel in human tumor cell lines in vitro.* Cancer Genomics-Proteomics, 2005. **2**(4): p. 219-226.

25. Moos, P.J. and F.A. Fitzpatrick, *Taxanes propagate apoptosis via two cell populations with distinctive cytological and molecular traits.* Cell Growth Differ, 1998. **9**(8): p. 687-97.

26. Mathew, P. and R. Dipaola, *Taxane refractory prostate cancer.* J Urol, 2007. **178**(3 Pt 2): p. S36-41.

27. Mediavilla-Varela, M., et al., *Docetaxel-induced prostate cancer cell death involves concomitant activation of caspase and lysosomal pathways and is attenuated by LEDGF/p75.* Mol Cancer, 2009. **8**: p. 68.

28. Sprowl, J.A., et al., *Alterations in tumor necrosis factor signaling pathways are associated with cytotoxicity and resistance to taxanes: a study in isogenic resistant tumor cells.* Breast Cancer Res, 2012. **14**(1): p. R2.

29. Bogdan, C. and A. Ding, *Taxol, a microtubule-stabilizing antineoplastic agent, induces expression of tumor necrosis factor alpha and interleukin-1 in macrophages.* J Leukoc Biol, 1992. **52**(1): p. 119-21.

30. Hestdal, K., et al., *Dysregulation of membrane-bound tumor necrosis factor-alpha and tumor necrosis factor receptors on mononuclear cells in human immunodeficiency virus type 1 infection: low percentage of p75-tumor necrosis factor receptor positive cells in patients with advanced disease and high viral load.* Blood, 1997. **90**(7): p. 2670-9.

31. Parameswaran, N. and S. Patial, *Tumor necrosis factor-alpha signaling in macrophages.* Crit Rev Eukaryot Gene Expr, 2010. **20**(2): p. 87-103.

32. MacEwan, D.J., *TNF ligands and receptors--a matter of life and death.* Br J Pharmacol, 2002. **135**(4): p. 855-75.

33. Davis, W., Jr., Z. Ronai, and K.D. Tew, *Cellular thiols and reactive oxygen species in drug-induced apoptosis.* J Pharmacol Exp Ther, 2001. **296**(1): p. 1-6.

34. Geng, C.X., Z.C. Zeng, and J.Y. Wang, *Docetaxel inhibits SMMC-7721 human hepatocellular carcinoma cells growth and induces apoptosis.* World J Gastroenterol, 2003. **9**(4): p. 696-700.

35. Vacca, A., et al., *Docetaxel versus paclitaxel for antiangiogenesis.* J Hematother Stem Cell Res, 2002. **11**(1): p. 103-18.

36. Kavallaris, M., et al., *Taxol-resistant epithelial ovarian tumors are associated with altered expression of specific beta-tubulin isotypes.* J Clin Invest, 1997. **100**(5): p. 1282-93.

37. Monzo, M., et al., *Paclitaxel resistance in non-small-cell lung cancer associated with beta-tubulin gene mutations.* J Clin Oncol, 1999. **17**(6): p. 1786-93.

38. Wang, Z., et al., *Differential effect of anti-apoptotic genes Bcl-xL and c-FLIP on sensitivity of MCF-7 breast cancer cells to paclitaxel and docetaxel.* Anticancer Res, 2005. **25**(3c): p. 2367-79.

39. Fukuda, S. and L.M. Pelus, *Survivin, a cancer target with an emerging role in normal adult tissues.* Mol Cancer Ther, 2006. **5**(5): p. 1087-98.

40. Zaffaroni, N., et al., *Expression of the anti-apoptotic gene survivin correlates with taxol resistance in human ovarian cancer.* Cell Mol Life Sci, 2002. **59**(8): p. 1406-12.

41. Fojo, T. and M. Menefee, *Mechanisms of multidrug resistance: the potential role of microtubule-stabilizing agents.* Ann Oncol, 2007. **18 Suppl 5**: p. v3-8.

42. Reed, K., et al., *Hypermethylation of the ABCB1 downstream gene promoter accompanies ABCB1 gene amplification and increased expression in docetaxel-resistant MCF-7 breast tumor cells.* Epigenetics, 2008. **3**(5): p. 270-80.

43. Armstrong, S.R., et al., *Distinct genetic alterations occur in ovarian tumor cells selected for combined resistance to carboplatin and docetaxel.* J Ovarian Res, 2012. **5**(1): p. 40.

44. Duan, Z., K.A. Brakora, and M.V. Seiden, *Inhibition of ABCB1 (MDR1) and ABCB4 (MDR3) expression by small interfering RNA and reversal of paclitaxel resistance in human ovarian cancer cells.* Mol Cancer Ther, 2004. **3**(7): p. 833-8.

45. Chang, H., et al., *Association of the ABCB1 gene polymorphisms 2677G>T/A and 3435C>T with clinical outcomes of paclitaxel monotherapy in metastatic breast cancer patients.* Ann Oncol, 2009. **20**(2): p. 272-7.

46. Harris, J.W., et al., *Isolation, structural determination, and biological activity of 6 alpha-hydroxytaxol, the principal human metabolite of taxol.* J Med Chem, 1994. **37**(5): p. 706-9.

47. McFadyen, M.C., W.T. Melvin, and G.I. Murray, *Cytochrome P450 enzymes: novel options for cancer therapeutics.* Mol Cancer Ther, 2004. **3**(3): p. 363-71.

48. Pastina, I., et al., *Cytochrome 450 1B1 (CYP1B1) polymorphisms associated with response to docetaxel in Castration-Resistant Prostate Cancer (CRPC) patients.* BMC Cancer, 2010. **10**: p. 511.

49. Hamilton, K.E., et al., *Cytokine induction of tumor necrosis factor receptor 2 is mediated by STAT3 in colon cancer cells.* Mol Cancer Res, 2011. **9**(12): p. 1718-31.

50. Das, G.C., et al., *Taxol-induced cell cycle arrest and apoptosis: dose-response relationship in lung cancer cells of different wild-type p53 status and under isogenic condition.* Cancer Lett, 2001. **165**(2): p. 147-53.

51. McBride, A. and S.K. Butler, *Eribulin mesylate: a novel halichondrin B analogue for the treatment of metastatic breast cancer.* Am J Health Syst Pharm, 2012. **69**(9): p. 745-55.

52. Kelling, J., et al., *Suppression of centromere dynamics by Taxol in living osteosarcoma cells.* Cancer Res, 2003. **63**(11): p. 2794-801.

53. Kenicer, J.E.M., J. Bartlett, and C. Gourley, *Investigation Into Taxane Resistant Breast Cancer*. 2011: University of Edinburgh.

54. Morse, D.L., et al., *Docetaxel induces cell death through mitotic catastrophe in human breast cancer cells.* Mol Cancer Ther, 2005. **4**(10): p. 1495-504.

55. Vakifahmetoglu, H., M. Olsson, and B. Zhivotovsky, *Death through a tragedy: mitotic catastrophe.* Cell Death Differ, 2008. **15**(7): p. 1153-62.

56. Roninson, I.B., E.V. Broude, and B.D. Chang, *If not apoptosis, then what? Treatment-induced senescence and mitotic catastrophe in tumor cells.* Drug Resist Updat, 2001. **4**(5): p. 303-13.

57. Blajeski, A.L., T.J. Kottke, and S.H. Kaufmann, *A multistep model for paclitaxel-induced apoptosis in human breast cancer cell lines.* Exp Cell Res, 2001. **270**(2): p. 277-88.

58. Craik, A.C., et al., *The BH3-only protein Bad confers breast cancer taxane sensitivity through a nonapoptotic mechanism.* Oncogene, 2010. **29**(39): p. 5381-91.

59. Bauer, J.A., et al., *Identification of markers of taxane sensitivity using proteomic and genomic analyses of breast tumors from patients receiving neoadjuvant paclitaxel and radiation.* Clin Cancer Res, 2010. **16**(2): p. 681-90.

60. Ferriss, J.S., et al., *Multi-gene expression predictors of single drug responses to adjuvant chemotherapy in ovarian carcinoma: predicting platinum resistance.* PLoS One, 2012. **7**(2): p. e30550.

61. Armstrong, D.K., *Relapsed ovarian cancer: challenges and management strategies for a chronic disease.* Oncologist, 2002. **7 Suppl 5**: p. 20-8.

62. Darshan, M.S., et al., *Taxane-induced blockade to nuclear accumulation of the androgen receptor predicts clinical responses in metastatic prostate cancer.* Cancer Res, 2011. **71**(18): p. 6019-29.

63. Eisenhauer, E.A., *Optimal assessment of response in ovarian cancer.* Ann Oncol, 2011. **22 Suppl 8**: p. viii49-viii51.

64. Eisenhauer, E.A., et al., *New response evaluation criteria in solid tumours: revised RECIST guideline (version 1.1).* Eur J Cancer, 2009. **45**(2): p. 228-47.

65. Wilkerson, J. and T. Fojo, *Progression-free survival is simply a measure of a drug's effect while administered and is not a surrogate for overall survival.* Cancer J, 2009. **15**(5): p. 379-85.

66. Gill, S. and D. Sargent, *End points for adjuvant therapy trials: has the time come to accept disease-free survival as a surrogate end point for overall survival?* Oncologist, 2006. **11**(6): p. 624-9.

67. Lobbes, M., R. Prevos, and M. Smidt, *Response monitoring of breast cancer patientsreceiving neoadjuvant chemotherapy using breast MRI – a review of current knowledge.* journal of Cancer Therapeutics and Research, 2012. **1**(1).

68. Weber, W.A., *PET for response assessment in oncology: radiotherapy and chemotherapy.* British Journal of Radiology, 2005. **Supplement_28**(1): p. 42-49.

69. Therasse, P., et al., *New guidelines to evaluate the response to treatment in solid tumors. European Organization for Research and Treatment of Cancer, National Cancer Institute of the United States, National Cancer Institute of Canada.* J Natl Cancer Inst, 2000. **92**(3): p. 205-16.

70. Su, H., et al., *Monitoring tumor glucose utilization by positron emission tomography for the prediction of treatment response to epidermal growth factor receptor kinase inhibitors.* Clin Cancer Res, 2006. **12**(19): p. 5659-67.

71. Lim, H.S., et al., *FDG PET/CT for the detection and evaluation of breast diseases: usefulness and limitations.* Radiographics, 2007. **27 Suppl 1**: p. S197-213.

72. Vimpeli, S.M., et al., *Large-core needle biopsy versus fine-needle aspiration biopsy in solid breast lesions: comparison of costs and diagnostic value.* Acta Radiol, 2008. **49**(8): p. 863-9.

73. Martin, R.C., 2nd, et al., *Is incisional biopsy of melanoma harmful?* Am J Surg, 2005. **190**(6): p. 913-7.

74. Pignata, S., et al., *Follow-up with CA125 after primary therapy of advanced ovarian cancer: in favor of continuing to prescribe CA125 during follow-up.* Ann Oncol, 2011. **22 Suppl 8**: p. viii40-viii44.

75. Azam, M., A. Qureshi, and S. Mansoor, *Comparison of estrogen receptors, progesterone receptors and HER-2/neu expression between primary and metastatic breast carcinoma.* J Pak Med Assoc, 2009. **59**(11): p. 736-40.

76. Miller, T.W., et al., *Hyperactivation of phosphatidylinositol-3 kinase promotes escape from hormone dependence in estrogen receptor-positive human breast cancer.* J Clin Invest, 2010. **120**(7): p. 2406-13.

77. Guiu, S., et al., *Predictive Factors of Response in HER2-Positive Breast Cancer Treated by Neoadjuvant Therapy.* J Oncol, 2013. **2013**: p. 854121.

78. Ross, J.S., et al., *Targeted therapy in breast cancer: the HER-2/neu gene and protein.* Mol Cell Proteomics, 2004. **3**(4): p. 379-98.

79. Jones, A., *Combining trastuzumab (Herceptin) with hormonal therapy in breast cancer: what can be expected and why?* Ann Oncol, 2003. **14**(12): p. 1697-704.

80. Samimi, G., et al., *TLE3 expression is associated with sensitivity to taxane treatment in ovarian carcinoma.* Cancer Epidemiol Biomarkers Prev, 2012. **21**(2): p. 273-9.

81. Sakuma, K., et al., *Pathological tumor response to neoadjuvant chemotherapy using anthracycline and taxanes in patients with triple-negative breast cancer.* Exp Ther Med, 2011. **2**(2): p. 257-264.

82. Parissenti, A.M., et al., *Association of low tumor RNA integrity with response to chemotherapy in breast cancer patients.* Breast Cancer Res Treat, 2010. **119**(2): p. 347-56.

83. Houseley, J. and D. Tollervey, *The many pathways of RNA degradation.* Cell, 2009. **136**(4): p. 763-76.

84. Houge, G., et al., *Selective cleavage of 28S rRNA variable regions V3 and V13 in myeloid leukemia cell apoptosis.* FEBS Lett, 1993. **315**(1): p. 16-20.

85. Hoat, T.X., et al., *Specific cleavage of ribosomal RNA and mRNA during victorin-induced apoptotic cell death in oat.* Plant J, 2006. **46**(6): p. 922-33.

86. Lafarga, M., et al., *Apoptosis induced by methylazoxymethanol in developing rat cerebellum: organization of the cell nucleus and its relationship to DNA and rRNA degradation.* Cell Tissue Res, 1997. **289**(1): p. 25-38.

87. King, K.L., et al., *28S ribosome degradation in lymphoid cell apoptosis: evidence for caspase and Bcl-2-dependent and -independent pathways.* Cell Death Differ, 2000. **7**(10): p. 994-1001.

88. Jordan, P. and M. Carmo-Fonseca, *Cisplatin inhibits synthesis of ribosomal RNA in vivo.* Nucleic Acids Res, 1998. **26**(12): p. 2831-6.

89. Burger, K., et al., *Chemotherapeutic drugs inhibit ribosome biogenesis at various levels.* J Biol Chem, 2010. **285**(16): p. 12416-25.

90. Laemmli, U.K., *Cleavage of structural proteins during the assembly of the head of bacteriophage T4.* Nature, 1970. **227**(5259): p. 680-5.

91. Markman, M., *Pharmaceutical management of ovarian cancer : current status.* Drugs, 2008. **68**(6): p. 771-89.

92. Prescott, D.M., *METHODS IN CELL BIOLOGY*. 1976: Elsevier Science.

93. Wang, X.P., et al., *Live morphological analysis of taxol-induced cytoplasmic vacuolization [corrected] in human lung adenocarcinoma cells.* Micron, 2008. **39**(8): p. 1216-21.

94. Neufeld, T.P. and B.A. Edgar, *Connections between growth and the cell cycle.* Curr Opin Cell Biol, 1998. **10**(6): p. 784-90.

95. Zhu, J., et al., *Centrosome impairments and consequent cytokinesis defects are possible mechanisms of taxane drugs.* Anticancer Res, 2005. **25**(3B): p. 1919-25.

96. Schroeder, A., et al., *The RIN: an RNA integrity number for assigning integrity values to RNA measurements.* BMC Mol Biol, 2006. **7**: p. 3.

97. Dumontet, C. and M.A. Jordan, *Microtubule-binding agents: a dynamic field of cancer therapeutics.* Nat Rev Drug Discov, 2010. **9**(10): p. 790-803.

98. He, K., H.R. Zhou, and J.J. Pestka, *Targets and intracellular signaling mechanisms for deoxynivalenol-induced ribosomal RNA cleavage.* Toxicol Sci, 2012. **127**(2): p. 382-90.

99. Houge, G., et al., *Fine mapping of 28S rRNA sites specifically cleaved in cells undergoing apoptosis.* Mol Cell Biol, 1995. **15**(4): p. 2051-62.

100. Pazdur, R., et al., *The taxoids: paclitaxel (Taxol) and docetaxel (Taxotere).* Cancer Treat Rev, 1993. **19**(4): p. 351-86.

101. Kovar, J., et al., *Comparison of cell death-inducing effect of novel taxane SB-T-1216 and paclitaxel in breast cancer cells.* Anticancer Res, 2009. **29**(8): p. 2951-60.

102. Hernandez-Vargas, H., J. Palacios, and G. Moreno-Bueno, *Molecular profiling of docetaxel cytotoxicity in breast cancer cells: uncoupling of aberrant mitosis and apoptosis.* Oncogene, 2007. **26**(20): p. 2902-13.

103. Kroemer, G., et al., *Classification of cell death: recommendations of the Nomenclature Committee on Cell Death 2009.* Cell Death Differ, 2009. **16**(1): p. 3-11.

104. Riccardi, C. and I. Nicoletti, *Analysis of apoptosis by propidium iodide staining and flow cytometry.* Nat Protoc, 2006. **1**(3): p. 1458-61.

105. Koopman, G., et al., *Annexin V for flow cytometric detection of phosphatidylserine expression on B cells undergoing apoptosis.* Blood, 1994. **84**(5): p. 1415-20.

106. van Engeland, M., et al., *Annexin V-affinity assay: a review on an apoptosis detection system based on phosphatidylserine exposure.* Cytometry, 1998. **31**(1): p. 1-9.

107. Bevers, E.M., P. Comfurius, and R.F. Zwaal, *Changes in membrane phospholipid distribution during platelet activation.* Biochim Biophys Acta, 1983. **736**(1): p. 57-66.

108. Yang, M.Y., et al., *Reversible phosphatidylserine expression on blood granulocytes related to membrane perturbation but not DNA strand breaks.* J Leukoc Biol, 2002. **71**(2): p. 231-7.

109. Li, Y., et al., *Regulation of microtubule, apoptosis, and cell cycle-related genes by taxotere in prostate cancer cells analyzed by microarray.* Neoplasia, 2004. **6**(2): p. 158-67.

110. Basturea, G.N., M.A. Zundel, and M.P. Deutscher, *Degradation of ribosomal RNA during starvation: comparison to quality control during steady-state growth and a role for RNase PH.* RNA, 2011. **17**(2): p. 338-45.

111. Hagisawa, S., T. Mikami, and Y. Sato, *Docetaxel-induced apoptosis in the mitotic phase: electron microscopic and cytochemical studies of human leukemia cells.* Med Electron Microsc, 1999. **32**(3): p. 167-174.

112. Fabbri, F., et al., *Sequential events of apoptosis involving docetaxel, a microtubule-interfering agent: a cytometric study.* BMC Cell Biol, 2006. **7**: p. 6.

113. Schulze-Osthoff, K., et al., *Cell nucleus and DNA fragmentation are not required for apoptosis.* J Cell Biol, 1994. **127**(1): p. 15-20.

114. Yamaguchi, K., et al., *Renal carcinoma cells undergo apoptosis without oligonucleosomal DNA fragmentation.* Biochem Biophys Res Commun, 2004. **318**(3): p. 710-3.

115. Long, J.S. and K.M. Ryan, *New frontiers in promoting tumour cell death: targeting apoptosis, necroptosis and autophagy.* Oncogene, 2012. **31**(49): p. 5045-60.

116. Mhaidat, N.M., et al., *Docetaxel-induced apoptosis in melanoma cells is dependent on activation of caspase-2.* Mol Cancer Ther, 2007. **6**(2): p. 752-61.

117. Boland, K., L. Flanagan, and J.H. Prehn, *Paracrine control of tissue regeneration and cell proliferation by Caspase-3.* Cell Death Dis, 2013. **4**: p. e725.

118. Wang, X.W., et al., *FG020326 sensitized multidrug resistant cancer cells to docetaxel-mediated apoptosis via enhancement of caspases activation.* Molecules, 2012. **17**(5): p. 5442-58.

119. Halder, J., et al., *Focal adhesion kinase silencing augments docetaxel-mediated apoptosis in ovarian cancer cells.* Clin Cancer Res, 2005. **11**(24 Pt 1): p. 8829-36.

120. Chauvier, D., et al., *Broad-spectrum caspase inhibitors: from myth to reality?* Cell Death Differ, 2007. **14**(2): p. 387-91.

121. He, K., H.R. Zhou, and J.J. Pestka, *Mechanisms for ribotoxin-induced ribosomal RNA cleavage.* Toxicol Appl Pharmacol, 2012. **265**(1): p. 10-8.

122. Lamkanfi, M., et al., *Caspases in cell survival, proliferation and differentiation.* Cell Death Differ, 2007. **14**(1): p. 44-55.

123. Malloy, P.J. and D. Feldman, *Inactivation of the human vitamin D receptor by caspase-3.* Endocrinology, 2009. **150**(2): p. 679-86.

124. Taylor, S.L., et al., *Somatic cell apoptosis markers and pathways in human ejaculated sperm: potential utility as indicators of sperm quality.* Mol Hum Reprod, 2004. **10**(11): p. 825-34.